Neotropical Ichthyology

Original article

https://doi.org/10.1590/1982-0224-2025-0178

urn:lsid:zoobank.org:pub:22443823-1CEA-4562-8B83-7EB876D9A522

A new species of freshwater stingray (Myliobatiformes: Potamotrygoninae) from northern South America

Devya Hemraj-Naraine[1,2], João Pedro Fontenelle[3], Astrid Acosta-Santos[4], Nathan R. Lovejoy[5], Elford Liverpool[6] and Matthew A. Kolmann[1]

Correspondence:
Matthew A. Kolmann
matthew.kolmann@louisville.edu

A new species of freshwater stingray (Potamotrygoninae) is described from the Demerara River, Guyana and río Guanare, Venezuela. It is distinguished from all other regional congeneric taxa (*i.e.*, *Potamotrygon marinae*, *P. schroederi*, *P. orbignyi*, *P. motoro*, and *P. boesemani*) by a combination of meristic, morphometric, and molecular evidence. Unlike *P. motoro* and *P. boesemani*, which exhibit distinct dorsal ocelli, and *P. schroederi*, which has numerous tan, yellow or orange rosettes on a dark background coloration, the new species *Potamotrygon siponinmorok*, does not have pigment organised in spots, exhibiting reticulated patterns more similar to *P. marinae* and *P. orbignyi*. However, the new species differs from these similarly patterned species (*i.e.*, *P. marinae* and *P. orbignyi*) by having a longer tail, fewer teeth, differently shaped teeth, and contrasting lateral line morphology. Molecular analysis corroborates *P. siponinmorok*, as a distinct lineage within the *Potamotrygon* clade, and its close relationship with *P. marinae* from the Eastern Guianas, *P. orbignyi* from the Orinoco, and *P. schroederi* from the rio Negro. This species description highlights the importance of thorough, complementary and integrative taxonomy studies for groups with pronounced morphological variability and levels of endemism, especially from areas under threat of habitat degradation.

Keywords: Guiana Shield, Integrative taxonomy, Marine-derived lineage, Morphology, South America.

Submitted July 14, 2025
Accepted December 23, 2025
Epub April 27, 2026

Associate Editor Bruno Melo
Section Editor William Crampton
Editor-in-chief José Birindelli

Online version ISSN 1982-0224
Print version ISSN 1679-6225

Neotrop. Ichthyol.
vol. 24, no. 1, 2026

---

1 Department of Biology, University of Louisville, Louisville, KY USA. (DHN) ddhemr01@louisville.edu, (MAK) matthew.kolmann@louisville.edu (corresponding author).

2 Center for the Study of Biological Diversity, University of Guyana, Guyana.

3 Institute of Forestry and Conservation, Daniels Faculty, University of Toronto, Toronto, ON Canada. (JPF) fontene3@gmail.com.

4 Instituto Amazónico de Investigaciones Científicas Sinchi, Leticia, Amazonas, Colombia. (AAS) astridacostasantos@gmail.com.

5 Department of Biological Sciences, University of Toronto Scarborough, Toronto, ON Canada. (NL) nathan.lovejoy@utoronto.ca.

6 Department of Biology, University of Guyana, Guyana. (EL) elford.liverpool@uog.edu.gy.

Uma nova espécie de arraia de água doce (Potamotrygoninae) é descrita do rio Demerara, Guiana, e do rio Guanare, Venezuela. Ela se distingue de todos os outros táxons congêneres regionais (i.e. *Potamotrygon marinae*, *P. schroederi*, *P. orbignyi*, *P. motoro* e *P. boesemani*) por uma combinação de evidências merísticas, morfométricas e moleculares. Ao contrário de *P. motoro* e *P. boesemani*, que exibem ocelos dorsais distintos, e *P. schroederi*, que possui numerosas rosetas castanhas, amarelas ou alaranjadas sobre uma coloração de fundo escuro, a nova espécie *Potamotrygon siponinmorok* não possui pigmento organizado em manchas, exibindo padrões reticulados mais semelhantes a *P. marinae* e *P. orbignyi*. No entanto, a nova espécie difere dessas espécies com padrões semelhantes (ou seja, *P. marinae* e *P. orbignyi*) por apresentar cauda mais longa, menos dentes, dentes com formatos diferentes e morfologia contrastante da linha lateral. A análise molecular corrobora *P. siponinmorok* como uma linhagem distinta dentro do clado *Potamotrygon* e sua estreita relação com *P. marinae* das Guianas Orientais, *P. orbignyi* do Orinoco e *P. schroederi* do rio Negro. Esta descrição da espécie destaca a importância de estudos taxonômicos completos, complementares e integrativos para grupos com pronunciada variabilidade morfológica e níveis de endemismo, especialmente em áreas sob ameaça de degradação de habitat.

Palavra-chave: América do Sul, Escudo das Guianas, Linhagem marinha, Morfologia, Taxonomia integrativa.

INTRODUCTION

Freshwater river systems in South America are some of the most diverse ecosystems on the planet, with a small but important portion of this diversity being fishes that invaded freshwater habitats from marine ecosystems (Lundberg *et al*., 2000; Lovejoy *et al*., 2009; Reis *et al*., 2016). These biological invasions of freshwaters coincide with several geographical marine incursions over the past 10–50 million years (Bloom, Lovejoy, 2017). For example, anchovies (Engraulidae; Bloom, Lovejoy, 2012) and needlefishes (Belonidae; Lovejoy, Collette, 2001) invaded South American freshwaters during the Oligocene, while pufferfishes (Tetraodontidae), drums/croakers (Sciaenidae), sea catfishes (Ariidae), and halfbeaks (Hemiramphidae) during the mid to late Miocene (Betancur, 2010; Yamanoue *et al*., 2011; Cooke *et al*., 2012; Lo *et al*., 2015; Bloom, Lovejoy, 2017). However, the oldest marine invasions of continental South America were accomplished by long-fin herrings (Pristigasteridae) and stingrays (Potamotrygoninae) during the Eocene (Bloom, Lovejoy, 2017; Fontenelle *et al*., 2021a; Kolmann *et al*., 2022). While some of these South American marine derived linages (MDL) have seen limited lineage diversification and number only several species (*e.g*., halfbeaks and pufferfishes; (Bloom, Lovejoy, 2017), freshwater stingrays or “river rays” have diversified in several basins all across South America (Lovejoy *et al*., 1998, 2006; Fontenelle *et al*., 2021b), with 39 currently valid species occurring in South America, seven in the La Plata basin, six in the Orinoco basin, and three species in the Guianas (Taphorn *et al*., 2022; Torres *et al*., 2022).

The stingrays in the Potamotrygonidae consist of two subfamilies: Potamotrygoninae and Styracurinae (Carvalho *et al*., 2016). The Styracurinae consists of two species of marine stingrays (*Styracura*) distributed on both sides of the Isthmus of Panama, in the East Pacific and Western Caribbean (Lovejoy, 1996, 1997). The subfamily Potamotrygoninae, consists of the Neotropical freshwater stingrays proper (Carvalho *et al*., 2016; Fontenelle *et al*., 2021a), which are one of the few extant, obligate freshwater elasmobranchs in the world (Araújo *et al*., 2004). Potamotrygoninae is composed of four genera: *Paratrygon* Duméril, 1865, *Plesiotrygon* Rosa, Castello & Thorson, 1987, *Potamotrygon* Garman, 1877 and *Heliotrygon* Carvalho & Lovejoy, 2011). *Potamotrygon* is the most diverse genus, with a total of 33 species (Rosa *et al*., 2008; Carvalho, Lovejoy, 2011; Loboda, Carvalho, 2013; da Silva, Carvalho, 2015; Fontenelle, Carvalho, 2017; da Silva, Loboda, 2019; Fontenelle *et al*., 2021a), or 32 species if *Potamotrygon roulini* Roberts, 2020 is excluded, as its validity as a distinct species has been questioned (da Silva *et al*., 2021). *Potamotrygon* is also the youngest of the four genera, diversifying around 18–22 million years ago, prior to the formation of the modern Amazon River (Fontenelle *et al*., 2021b; Kolmann *et al*., 2022). Beyond exhibiting high species richness, *Potamotrygon* also accounts for a significant proportion of the ecological and phenotypic diversity within Potamotrygoninae (Fontenelle *et al*., 2018, 2021b; Kolmann *et al*., 2022).

Potamotrygon species vary widely in size, from under 0.25 m to greater than 1 m in disk width, and exhibit diverse trophic specializations, including insectivory, crustacivory, and molluscivory, throughout the Amazon and adjacent basins (Moro, 2010; Rutledge *et al*., 2019; Kolmann *et al*., 2022). Additionally, their chromatic phenotypes are likewise diverse, which has made them sought-after commodities within the global ornamental aquarium trade (Beltrão *et al*., 2021). However, this polymorphism in coloration has often resulted in misidentification of *Potamotrygon* species, especially because many species are polychromatic (multiple distinct phenotypes within a species) (*e.g*., *Potamotrygon orbignyi* Castelnau, 1855, *P. motoro* Müller & Henle, 1841). Taxonomic appraisal of this subfamily is hindered by polychromatism, polymorphism, poor specimen availability and curation, as well as molecular paraphyly (Fontenelle *et al*., 2021b) within widespread species such as *P. orbignyi*. This phenotypic and genotypic variability likely stems from a complex history of hybridization, incomplete lineage sorting, convergent evolution, and rapid diversification, as well as curatorial issues like misidentification (Toffoli *et al*., 2008; Fontenelle *et al*., 2021a,b; Torres *et al*., 2022). For example, individuals of *P. orbignyi* often cluster phylogenetically with sympatric congeners, rather than with conspecifics from river basins (Carvalho *et al*., 2016; Fontenelle *et al*., 2021a). Likewise, close relatives may exhibit geographically disjunct distributions that could reflect genuine phylogeographical and biogeographical divergence or instead arise from incomplete sampling or unrecognized (cryptic) lineages (Fontenelle *et al*., 2021a,b).

Consequently, the genus *Potamotrygon* is taxonomically complex, with molecular studies revealing numerous lineages that do not correspond to currently recognized taxonomic names (see Fontenelle *et al*., 2021b). This complexity has driven a surge of new species descriptions over the past two decades, supported by both detailed morphological analyses (*e.g*., Loboda, Carvalho, 2013; Fontenelle *et al*., 2014; da Silva, Carvalho, 2015; Fontenelle, Carvalho, 2017) and molecular evidence (Toffoli *et al*., 2008; Garcia *et al*., 2015; Fontenelle *et al*., 2021b). In this manuscript, we build on this framework by combining traditional morphometrics and meristics, morphospace analyses, and molecular evidence to describe a new species from the Demerara River (Guyana) and the río Guanare, (Venezuela), previously reported elsewhere as *Potamotrygon* cf. *orbignyi*, *Potamotrygon* sp. n. *orbignyi* (Fontenelle *et al*., 2021b) or *Potamotrygon* "Demerara" (Kolmann *et al*., 2022). Beyond its formal description, we evaluate its phylogenetic placement within *Potamotrygon*, clarify its distinction from closely related taxa, and provide an updated account of its distribution and ecological range. Finally, we discuss the broader implications of this discovery for understanding species diversity, taxonomy, and biogeography of freshwater stingrays in northern South America.

MATERIAL AND METHODS

Specimen collection. Ten specimens were collected from two localities along the Demerara River, Guyana (6.543444, -58.243833 to 6.821667, -58.183778; Fig. 1; Tab. **S1**) in March 2015 using fishermen's pin seines and gillnets. Specimens were euthanized using clove oil following the immersion protocol of Ferreira *et al.* (2019). Muscle tissue was preserved in 95% ethanol for DNA extraction, and specimens were subsequently fixed in buffered 10% formalin and stored in 70% ethanol. All specimens were deposited and accessioned at the Royal Ontario Museum, Toronto, Canada. In addition, a single specimen previously identified as *P. orbignyi* (ROM 8998/AUM 53789) from the Auburn University Natural History Museum Fish Collection, collected in March 2010 from río Guanare, Venezuela (8.91411 -69.76110), was examined as it was recovered clustered with *Potamotrygon* sp. n. *orbignyi* (Fontenelle *et al*., 2021b).

A total of 26 morphometrics and 13 meristic measurements were taken, adapted from Rosa (1985) (Fig. 2; Tab. 1–2). Internal morphology (*e.g*., skeletal characters) was visualized from 2D radiographed specimens using a General Electric GE-DXS 350, Faxitron model 43805N (GE Healthcare Technologies, Inc., Chicago, Illinois, USA) with a Carestream Industrex HPX-1 detector (Carestream Health, Rochester, New York, USA). High-resolution digital photographs of both dorsal and ventral aspects were captured for the holotype (CSBD F3620 [olim ROM 100073] ROM T20846) and paratypes using a Nikon D3200 24.2 MP CMOS Digital SLR camera. Additionally, detailed images of the dermal denticles, mouth, upper and lower jaws were obtained for the holotype. A transparent plastic sheet was placed on the ventral section and was used to trace the lateral line, which was visible on the ventral surface. The terminology used to distinguish each canal was adopted from Garman (1888) and Ewart, Mitchell (1892). Males were considered to be mature if they had fully developed, calcified claspers, while immature males had shorter, flexible, and uncalcified claspers (Pedreros-Sierra, Ramírez-Pinilla, 2015). Females were identified by the absence of claspers and sexual maturity was estimated using species-specific disk width (DW) thresholds as a proxy, following published estimates for Neotropical *Potamotrygon* species (*e.g*., *P. orbignyi*: ~244–260 mm DW, Carvalho, 2016; *P. motoro*: 310–440 mm DW, Deynat, 2006). All specimens used in this study are accessioned and housed at either the Academy of Natural Sciences of Philadelphia, Drexel University (ANSP); Auburn University Museum of Natural History, Auburn (AUM); Centre for the Study of Biological Diversity, University of Guyana, Georgetown (CSBD); Museo de Ciencias Naturales de la UNELLEZ, Guanare

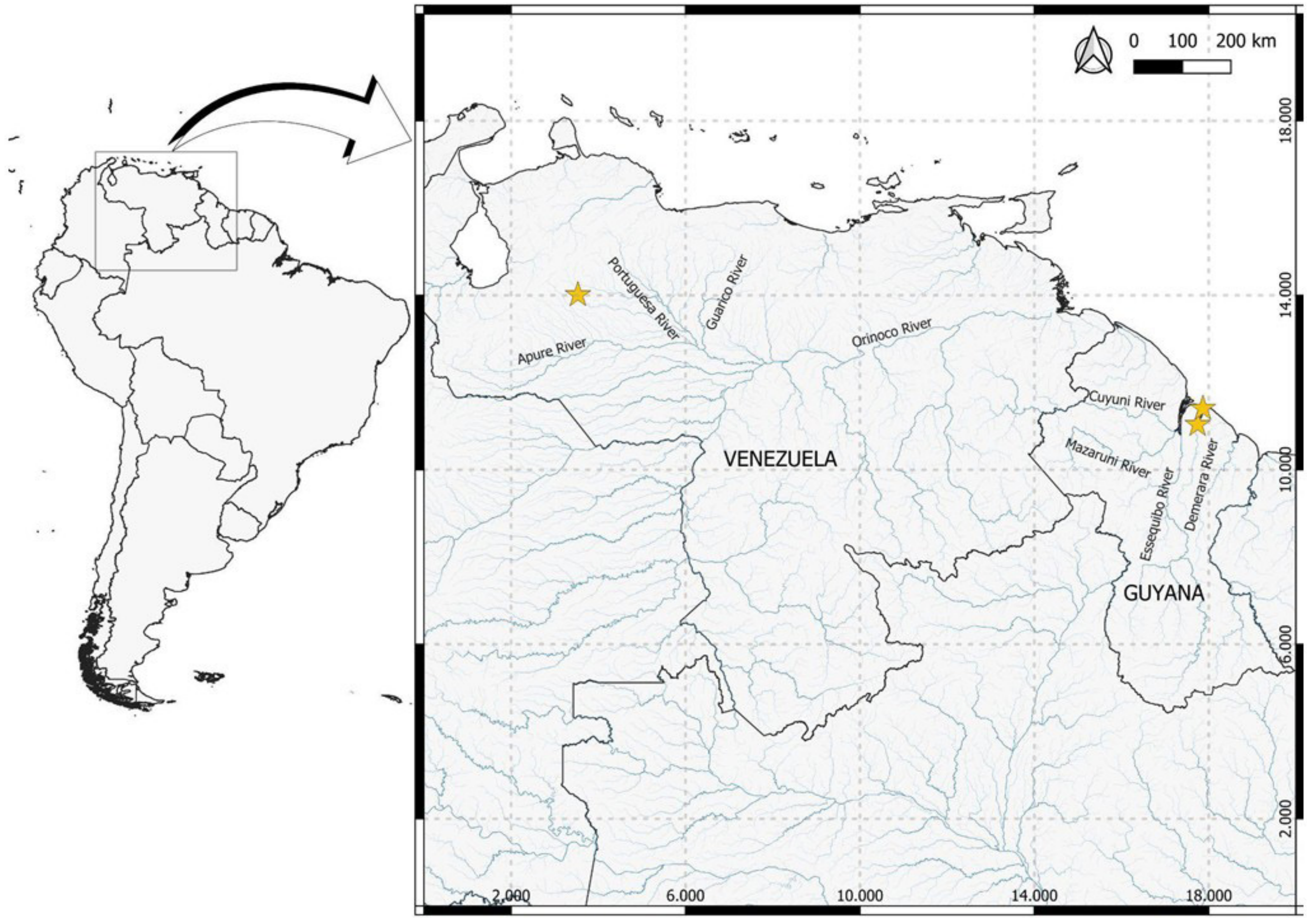

FIGURE 1 | The type locality where *Potamotrygon siponinmorok* has been recorded, collection sites are indicated by star symbols. Shapefile, copyright (c) 2021 Ujaval Gandhi.

(MCNG); Muséum National d'Histoire Naturelle, Paris (MNHN); Universidade Federal da Paraíba, João Pessoa (UFBP); Museu de Zoologia da Universidade de São Paulo, São Paulo (MZUSP); Royal Ontario Museum, Toronto (ROM); Smithsonian Museum of Natural History, Washington D.C. (USNM); University of Michigan Museum of Zoology, Ann Arbor (UMMZ), and Museum für Naturkunde, Berlin (ZMB).

Morphological analysis. Twenty-six morphometric characters were used to quantify differences in body shape and proportions among different *Potamotrygon* specimens, following da Silva (2015) (Fig. 2). Each morphometric measurement was then converted to a percentage relative to the specimen's disk width (%DW) (Tab. 2). To visualize species separation in morphospace using Principal Component Analysis (PCA), morphometric data were processed using the missMDA package (v. 1.19) (Josse, Husson, 2016) in R (v. 4.4.3) (Dalgaard, 2024). First, morphometric data were cleaned by removing non-numeric columns, and then missing values were imputed using imputed PCA. The optimal number of dimensions for imputation was estimated using the *estim_ncpPCA* function, and the missing values were then imputed via regularized PCA with *imputePCA* (ncp = 5). The resulting dataset was log-transformed to eliminate

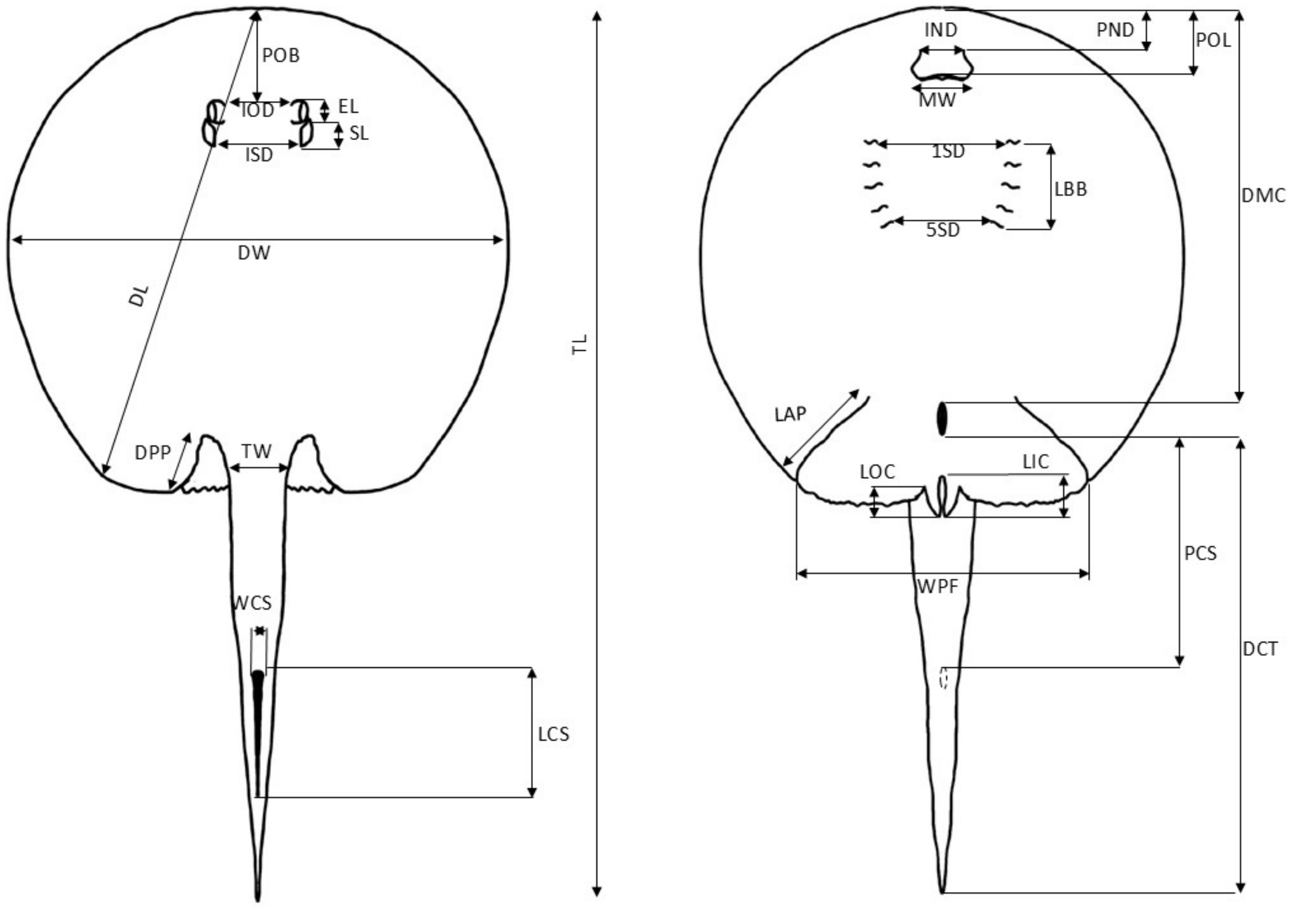

FIGURE 2 | Twenty-size (26) morphometrics collected for all type materials. TL, total length; DL, disk length; DW, disk width; IOD, interorbital distance; EL, eye length; SL, spiracles length; PND, prenasal distance; POL, preoral distance; MW, mouth width; 1SD, distance between the first pair of gill slits; 5SD, distance between the fifth pair of gill slits; LBB, length of branchial basket; LAP, length of the anterior margin of the pelvic fin; WPF, width of the pelvic fin (combined); LOC, length of the outer margin of the clasper; LIC, length of the inner margin of the clasper; DCT, center distance of posterior margin of the cloaca and the tip of the tail; TW, tail width; DMC, center distance tip of the muzzle to the anterior margin of the cloaca; DPP, distance between the insertion of the pectoral fins to the posterior margin of the pelvic fin; PCS, posterior margin of the cloaca to the anterior margin of the serrated thorn; POB, preorbital distance; LCS, length of caudal sting; WCS, width of the caudal sting; ISD, interspiracle distance; IND, internasal distance. Adapted from da Silva (2015).

skewness and PCA analysis was performed using the *prcomp* function. The first three principal components were retained, and the percentage of variance explained by each was calculated. Group labels (species or populations) and specimen identifiers were appended to the PCA scores for plotting. Two PCA plots were created using the ggplot2 package (v. 3.5.2) (Wickham, 2016). The first plot included nine *Potamotrygon* species found in the Guianas (Tab. 3) and nearby basins, and was used to assess overall morphological differentiation among species based on shape variables. The second plot focused on a subset of species that were morphologically similar but differed in coloration. We included *Potamotrygon* sp. (Mahaica) and *Potamotrygon* sp. in both plots. These taxa differ in coloration and minute morphological features and were therefore treated as separate species. All statistical analyses were performed in R v. 4.4.3.

TABLE 1 | Morphometric values of specimens of *Potamotrygon siponinmorok*. DW: disk width; SD: Standard deviation; N: number of individuals. See Fig. 1 for morphometric descriptions. *Measurement was derived from images. Morphometrics for *P. orbignyi* were collected from da Silva, Carvalho (2015).

Parameters	*Potamotrygon siponinmorok*									*Potamotrygon orbignyi*				
	N	Holotype		Range paratype		Mean		SD		N	Total Range		Mean	SD
		mm	%DW	mm	%DW	mm	%DW	mm	%DW		mm	%DW	%DW	%DW
Total length	10	456	203.6	358–725	192.1–211.8	451.0	211.7	116.2	22.3	291	171–1100	119.6–232.7	185.6	4
Disc length	10	245	109.4	177–358	99.6–109.4	229.1	108.0	55.3	13.5	291	108–700	101–122	109.9	0.5
Disc width	10	224		169–353	100–100	220.5		56.1		291	91–610			
Interorbital distance	10	48	21.4	34–73	18.7–21.4	44.1	20.7	11.9	2.7	291	11–75	8.5–19.5	12.2	0.6
Interspiracular distance	10	44	19.6	33–71	18.1–20.7	42.5	19.9	11.5	2.5	291	21–102	15.8–23.5	17.9	0.4
Eye length	10	9	4.0	8–12	3.4–5.3	9.0	4.3	1.2	0.7	291	5-16	2.4–7.4	4.1	0.2
Spiracle length	10	13	5.8	13–30	5.7–9.1	17.4	8.1	5.3	1.0	291	9-65	5.9–13.5	9.8	0.2
Preorbital length	9	53	23.7	42–60	21.4–24.9	47.7	21.8	6.7	8.3	291	21–150	17.1–28.3	23.3	0.4
Prenasal length	10	33	14.7	27–57	13.6–17.1	33.9	16.0	8.8	2.1	291	15–85	6.1–20.9	14.2	0.3
Preoral length	10	50	22.3	37–79	19.9–22.9	47.9	22.5	12.3	2.6	291	22–117	10.9–26.8	20.1	0.4
Internarial distance	10	18	8.0	11–25	6–8.9	16.8	7.9	4.0	1.1	291	8-50	5–11.1	7.9	0.2
Mouth width	10	18	8.0	12–29	6.6–8.9	17.7	8.3	4.9	1.2	291	8-57	5–13.1	8.5	0.2
Distance between 1st gill slits	10	55	24.6	41–94	21.6–26.6	53.7	25.0	16.2	2.7	291	22–158	19.4–29.6	24.4	0.3
Distance between 5th gill slits	10	41	18.3	30–78	16.8–22.1	40.2	18.6	14.5	2.5	291	14–105	11.9–21.7	15.9	0.3
Branchial basket length	10	40	17.9	29–60	15.9–23.7	39.9	18.9	8.8	2.9	291	17–120	14.8–22.9	18.5	0.2
Pelvic fin anterior margin length	10	52	23.2	38–93	17.9–26.4	50.8	23.6	16.1	2.1	291	18–120	14.3–31.3	22.8	0.3
Pelvic fins width	5			100–203	56.8–59.2	143.4	51.5	38.6	26.4	291	18–370	4.9–67.6	57.2	2
Clasper external length	6	12	5.4	8–22	4.2–8.7	13.2	6.5	6.3	3.0	170	3-73	2.4–25.6	10.6	1.4
Clasper internal length	6	19	8.5	12–34	6.8–12.5	19.2	9.3	8.6	3.2	170	8–133	6.6–33.2	20.1	2.1
Distance between cloaca and tail tip	10	257	114.7	204–406	110–120.9	256.6	120.7	63.3	12.8	291	81–540	68.9–141.1	92	2.9
Tail width	10	33	14.7	20–42	10.5–24.9	30.0	14.3	8.2	4.2	291	9-70	6–21.2	11.7	0.4
Snout to cloaca distance	10	198	88.4	146–332	80.9–94.1	190.0	88.8	56.3	11.4	291	86–575	79.7–137.2	88.3	2.1
Pectoral to posterior pelvic length	10	22	9.8	17–33	9.1–13.5	23.9	11.4	6.1	2.7	291	4-55	3.4–20.4	8.7	0.4
Distance from cloaca to sting origin	10	104	46.4	75–193	44.1–54.7	106.2	49.2	35.8	6.5	291	37–340	33.6–64	49.6	0.8
Sting length	10	52	23.2	35–76	15.4–25.7	46.2	21.9	11.3	3.3	291	21–150	9.4–31.3	21.3	0.4
Sting width	10	4	1.8	3–7	1.5–2.2	4.0	1.9	1.2	0.4	291	2-10	1.2–3.7	2	1

Nomenclature abbreviations. Morphometrics: TL, total length; DL, disk length; DW, disk width, IOD, interorbital distance; EL, eye length; SL, spiracle length; PND, prenasal distance; POL, preoral distance; MW, mouth width, 1SD, distance between the 1st pair of gill slits; 5SD, distance between the 5th pair of gill slits; LBB, length of branchial basket; LAP, length of the anterior margin of the pelvic fin; WPF, width of the pelvic fin (combined); LOC, length of the outer margin of the clasper, LIC, length of the inner margin of the clasper; DCT, posterior margin of the cloaca and the tip of the tail; TW, tail width; DMC, center distance tip of the rostral to the anterior margin of the cloaca; DPP, distance between the insertion of the pectoral fins to the posterior margin of the pelvic fin; PCS, posterior margin of the cloaca to the anterior margin of the serrated thorn; POB, preorbital distance; LCS, length of caudal sting; WCS, width of the caudal sting; ISD, interspiracle distance; IND, internasal distance. Lateral line system: AST, anterior sub pleural tubules; HYC, hyomandibular canal; IOL, infraorbital loop; JCH, jugular component of the hyomandibular canal; JUG, jugular canal; NAS, nasal canal; PJL, posterior jugular loop; SOL, suborbital loop; SPC, subpleural component of the hyomandibular canal; SPL, subpleural loop. Mouth, teeth and oral papillae (adapted from de Aquino *et al*., 2023): UT, upper teeth; LT, lower teeth; UL, upper lip; LL, lower lip; LG, lip groove; RL, Rostrum labium; OP, oral papillae. Claspers: AG, apopyle; CG, clasper groove; HG, hypopyle; PS, dorsal pseudosiphon; VPS, ventral pseudosiphon. *Skeletal anatomy*: AAC, anterior angular cartilage; BP, basipterygium; COB: coracoid bar; HYO, hyomandibula; MC, Meckel's cartilage; MES, mesopterygium; MET, metapterygium; MSC, mesocondyle; MTC, metacondyle; PIB, puboischiadic bar; PRO, propterygium; PRC, procondyle; PQ, palatoquadrate.

TABLE 2 | Meristic data for *Potamotrygon siponinmorok* and *P. orbignyi*. Meristics for *P. orbignyi* were collected from da Silva, Carvalho (2015). SD = Standard deviation.

Counts	*Potamotrygon siponinmorok*						*Potamotrygon orbignyi*			
	N	Holotype	Range	Mean	SD	Mode	N	Range	Mean	SD
Precaudal vertebrae	6	32	28–32	30.2	1.3	30	51	22–33	28.4	1.7
Caudal vertebrae	6	99	98–104	101.0	2.4	–	51	91–104	97.1	3.2
Total vertebrae	6	131	129–134	131.2	1.7	131	51	118–133	125.5	3.4
Diplospondylous vertebrae	6	95	90–96	93.7	2.1	94	51	85–99	91.5	3.6
Caudal sting vertebrae	5	74	74–80	76.2	2.7	74	51	–	–	–
Upper tooth row	2	28	27–28	27.5	0.70	–	53	26–44	35.3	4
Lower tooth row	2	35	26–35	30.5	6.36	–	53	24–45	33.6	4.9
Propterygial radials	6	48	44–48	45.8	1.8	48	51	40–46	43.5	1.4
Mesopterygial radials	6	15	15–20	16.7	2.0	15	51	13–17	15	1
Metapterrygial radials	6	38	21–39	35.0	7.0	39	51	26–39	36.8	1.8
Total pectoral radials	6	101	86–101	97.5	5.8	101	51	90–101	95.5	2.1
Pelvic radials (Male)	3	16	16–21	18.7	2.5	–	28	19–22	20.1	0.8
Pelvic radials (Female)	3	–	20–21	21.3	1.5	–	23	22–25	24.5	0.7

TABLE 3 | *Potamotrygon* spp. used in each morphological PCA analysis. Nine species were used to produce PCA (Fig. 11), while five species were used to produce PCA (Fig. 12).

Species	Full data set (Fig. 11)	Partial data set (Fig. 12)
Potamotrygon siponinmorok	✓	✓
Potamotrygon marinae	✓	✓
Potamotrygon orbignyi	✓	✓
Potamotrygon sp. (Mahaica)	✓	✓
Potamotrygon sp.	✓	✓
Potamotrygon scobina	✓	
Potamotrygon adamastor	✓	
Potamotrygon schroederi	✓	
Potamotrygon boesemani	✓	

DNA Barcoding & Gene Tree Inference. A total of 84 cytochrome c oxidase subunit I (COX1) gene sequences were obtained from GenBank (Tab. 4), representing multiple species of *Potamotrygon*, including previously published sequences from the new species (referred to as "*Potamotrygon orbignyi* ex Demerara River" and "*Potamotrygon* sp. ex Demerara River" in Fontenelle *et al*., 2021b:391 "Potamotrygon orbignyi ex Demerara River" and "Potamotrygon sp. ex Demerara River"). Our dataset included three individuals each of *P. adamastor* Fontenelle & Carvalho, 2017, *P. amandae* Loboda & Carvalho, 2013, *P. boesemani* Rosa, Carvalho & Almeida Wanderley, 2008 and *P. humerosa* Garmin, 1913; seven *Potamotrygon* sp.; four individuals of *P. siponinmorok* (including the holotype); four individuals each of *P. leopoldi* Castex & Castello, 1970 and *P. marinae* Deynat, 2006; eight of *P. motoro*; 38 of *P. orbignyi*; three of *P. schroederi* Fernández-Yépez, 1958; two of *P. scobina* Garman, 1913 and two *Potamotrygon* cf. *orbignyi* (Tab. 4). These sequences were selected based on their geographic distribution across 27 South American drainages and their genetic similarity to *P. siponinmorok*, as described by Fontenelle *et al*. (2021b). Sequence alignment was conducted using Multiple Sequence Alignment in CLUSTALW v. 2.1 (Larkin *et al*., 2007). Pairwise alignment parameters were set as follows: gap opening penalty = 15, gap extension penalty = 6.6, and weight matrix = ClustalW (for DNA). Multiple sequence alignment parameters were set as follows: gap opening penalty =15, gap extension penalty = 6.66, and hydrophilic gap penalties = Yes, transition weighting = No, and the weight matrix was set to ClustalW (for DNA). The aligned FASTA file was subsequently uploaded to the IQ-TREE web server (accessed: March 2025) for phylogenetic analysis using Maximum Likelihood (ML) as the optimality criterion. The parameters were set as follows: FreeRate heterogeneity model, ultrafast bootstrap analysis with 1,000 bootstrap replicates, maximum iterations = 1,000, minimum correlation coefficient = 0.99, SH-aLRT branch test with 1,000 replications, perturbation strength = 0.5, and the IQ-TREE stopping rule set to 100.

TABLE 4 | Vouhcer and accession information for samples of *Potamotrygon* spp. used in this study, including 84 cytochrome c oxidase subunit I (COX1) gene sequences downloaded from Genbank.

Species	Catalog/Tissue numbers	Accession number
Potamotrygon adamastor	AM07-45/MZUSP 104662	MW475782
Potamotrygon adamastor	AM07-46/MZUSP 104663	MW475783
Potamotrygon adamastor	AM07-47/MZUSP 104664	MW475784
Potamotrygon amandae	PU09-01/MZUSP 110849	MW475896
Potamotrygon amandae	PU09-34/MZUSP 110876	MW475915
Potamotrygon amandae	PU09-41/MZUSP 110883	MW475919
Potamotrygon boesemani	NL 10800/ROM 91269	MW475862
Potamotrygon boesemani	NL 11830	MW475867
Potamotrygon boesemani	NL 11831	MW475868
Potamotrygon siponinmorok	NL10110/ROM 103015a	MW475855
Potamotrygon siponinmorok	NL10111/ROM 103015b	MW475856
Potamotrygon siponinmorok	ROM T20846/ROM 100073a	MW475980
Potamotrygon siponinmorok	ROM T8998/AUM 53789	MW475974
Potamotrygon humerosa	AM07-21/MZUSP 104642	MW475759
Potamotrygon humerosa	AM07-22/MZUSP 115220	MW475760
Potamotrygon humerosa	TJ05_23/MZUSP 103913	MW476002
Potamotrygon leopoldi	BR96-135	MW475728
Potamotrygon leopoldi	TO05-68	MW476036
Potamotrygon leopoldi	TO05-89/MZUSP 104452	MW476041
Potamotrygon leopoldi	TO05-90/MZUSP 116090	MW476042
Potamotrygon marinae	NL 11827	MW475864
Potamotrygon marinae	NL 11828	MW475865
Potamotrygon marinae	NL 11829	MW475866
Potamotrygon marinae	ROM T18876/ROM 97978	MW475978
Potamotrygon motoro	PU09-26/ MZUSP 110873	MW475907
Potamotrygon motoro	PU09-36/ MZUSP 110878	MW482347
Potamotrygon motoro	PU09-37/ MZUSP 110878	MW475916
Potamotrygon motoro	RN05-63	MW475949
Potamotrygon motoro	RN11-43	MW475963
Potamotrygon motoro	RN11-44	MW475964
Potamotrygon motoro	RN11-52	MW475965
Potamotrygon motoro	TO 05-19/UNT7154	MW476024
Potamotrygon sp.	NL 00931	MW475845
Potamotrygon sp.	ROM T20689/ROM 100993	MW475979
Potamotrygon sp.	ROM T08361/ROM 87341	MW475973
Potamotrygon sp.	ROM T18145/ROM 97210	MW475977
Potamotrygon sp.	ROM T6650/ROM 86428a	MW475966
Potamotrygon sp.	ROM T6662/ROM 86428b	MW475967
Potamotrygon sp.	ROM T6861/ROM 86427	MW475968
Potamotrygon orbignyi	AC06-094/MZUSP 104028	MW475751
Potamotrygon orbignyi	AC06-096/MZUSP 117796	MW475751

➡

TABLE 4 | (Continued)

Species	Catalog/Tissue numbers	Accession number
Potamotrygon orbignyi	AM07-23/MZUSP 104643	MW475761
Potamotrygon orbignyi	AM07-24/MZUSP 115186	MW475762
Potamotrygon orbignyi	AM07-26/MZUSP 115187	MW475764
Potamotrygon orbignyi	AM07-27/MZUSP 104645	MW475765
Potamotrygon orbignyi	AM07-28/MZUSP 115188	MW475766
Potamotrygon orbignyi	AM07-34/MZUSP 104651	MW475772
Potamotrygon orbignyi	AM07-36/MZUSP 104653	MW475774
Potamotrygon orbignyi	AM07-39/MZUSP 104656	MW475777
Potamotrygon orbignyi	AM07-43/MZUSP 104660	MW475781
Potamotrygon orbignyi	AM07-50/MZUSP 104667	MW475787
Potamotrygon orbignyi	BR96-128	MW475726
Potamotrygon orbignyi	BR96-184/UFBP3536	MW475732
Potamotrygon orbignyi	JU12-08/MZUSP 117345	MW475812
Potamotrygon orbignyi	NL 02601	MW475850
Potamotrygon orbignyi	PA03-61/MZUSP 104275	MW475883
Potamotrygon orbignyi	PA03-62/MZUSP 104276	MW475884
Potamotrygon orbignyi	PU 09-04/MZUSP 117260	MW475897
Potamotrygon orbignyi	PU09-46/MZUSP 117264	MW475922
Potamotrygon orbignyi	RN05_59/MZUSP 117265	MW475947
Potamotrygon orbignyi	RN05-13/MZUSP 104971	MW475939
Potamotrygon orbignyi	RN05-50	MW475946
Potamotrygon orbignyi	RN 11-25	MW475958
Potamotrygon orbignyi	RN 11-26	MW475959
Potamotrygon orbignyi	RN 11-27	MW475960
Potamotrygon orbignyi	ROM T6965/ROM 85940	MW475969
Potamotrygon orbignyi	TA06-18/MZUSP 104989	MW475992
Potamotrygon orbignyi	TJ05_13/MZUSP 103906	MW475997
Potamotrygon orbignyi	TJ05_25	MW476003
Potamotrygon orbignyi	TO04-02/MZUSP 104388	MW476008
Potamotrygon orbignyi	TO04-03/MZUSP 115182	MW476009
Potamotrygon orbignyi	TO04-09/MZUSP 115184	MW476010
Potamotrygon orbignyi	TO05-38/MZUSP 104407	MW476032
Potamotrygon orbignyi	TO05-62/MZUSP 104429	MW476035
Potamotrygon orbignyi	TO05-81/MZUSP 104446	MW476039
Potamotrygon orbignyi	TO05-82/MZUSP 115193	MW476040
Potamotrygon orbignyi	VZ13-01/MCNG 56440	MW476048
Potamotrygon cf. *orbignyi*	JU12-11/MZUSP 117345	MW475812
Potamotrygon cf. *orbignyi*	AM07-33/MZUSP 104650	MW475771
Potamotrygon schroederi	RN05-01/MZUSP 117263	MW475936
Potamotrygon schroederi	RN 11-24	MW475957
Potamotrygon cf. *schroederi*	ROM T9542/AUM 54482	MW475975
Potamotrygon scobina	BR96-125/UFBP 3532	MW475723
Potamotrygon cf. *scobina*	NL 10116/ROM 103020	MW475859

RESULTS

Potamotrygon siponinmorok, new species

urn:lsid:zoobank.org:act:AF936050-68B1-4CD7-895B-D93827F4EE29

(Figs. 3–4F, 5–11; Tab. 1)

Potamotrygon orbignyi. —Fontenelle *et al*., 2021b:391, fig. 6 (CPC - Clade A).

Potamotrygon sp. —Fontenelle *et al*., 2021b:391, fig. 6 (CPC - Clade A).

Potamotrygon sp. 'Demerara'. —Kolmann *et al*., 2022:427, tab.1 (Summary of sources for potamotrygoninae dietary information from literature).

Holotype. CSBD F3620 (olim ROM 100073) ROM T20846, juvenile male, 224 mm DW; Demerara River, Guyana, 6.543444 -58.243833, Mar 2015, M. Kolmann, A. Little, E. Liverpool, S. Steele, N. Mangra & D. Gordon (Fig. 3A).

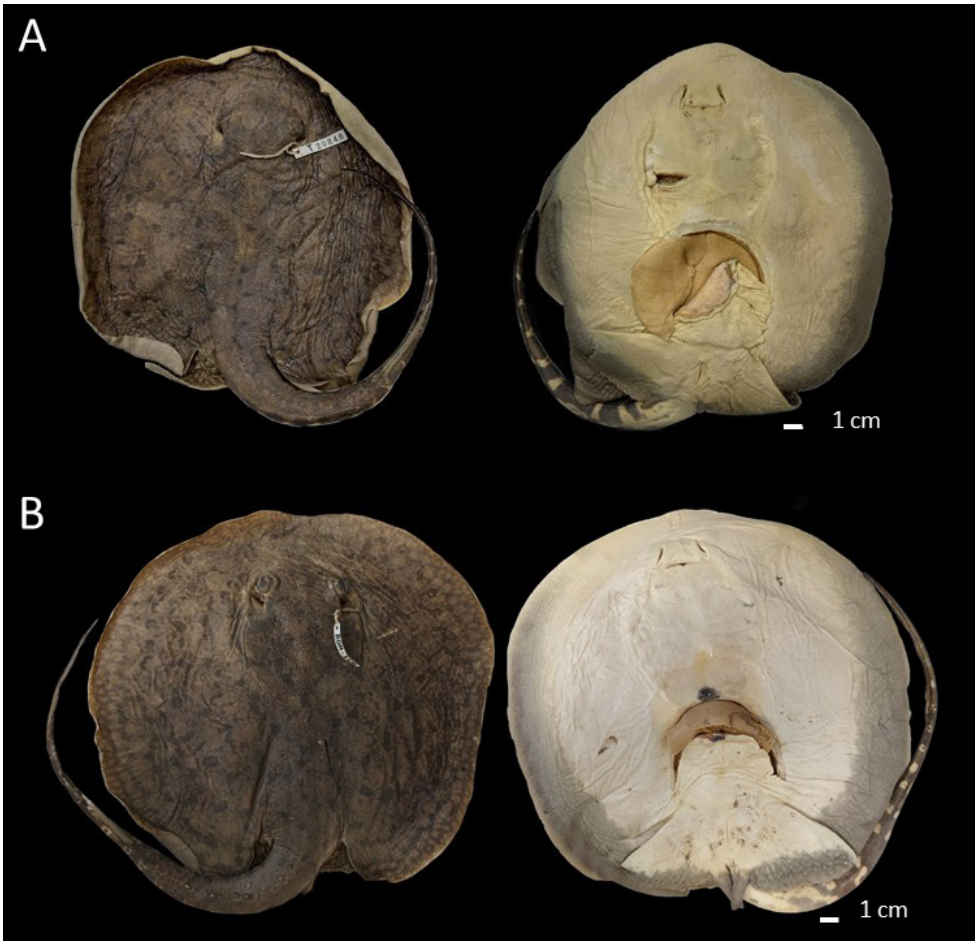

FIGURE 3 | **A.** Holotype of *Potamotrygon siponinmorok*, CSBD F3620 (juvenile male, 224 mm DW), dorsal and ventral view. **B.** Paratype of *Potamotrygon siponinmorok*, ROM 100073-20848 (juvenile male, 272 mm DW), dorsal and ventral view.

Paratypes. Demerara River, Guyana. ROM 100073-20848 (juvenile male, 272 mm DW) (Fig. 3B), Demerara River, Guyana, 6.543444 -58.243833, Mar 2015, M. Kolmann, A. Little, E. Liverpool, S. Steele, N. Mangra & D. Gordon. ROM 103015-NL10110 (juvenile female, 169 mm DW), Demerara River, Guyana, 6.543444 -58.243833, Mar 2015, M. Kolmann, A. Little, E. Liverpool, S. Steele, N. Mangra & D. Gordon. ROM 100992-20688 (adult female, 353 mm DW), Demerara River, 6.821667 -58.183778, Mar 2015, M. Kolmann, A. Little, E. Liverpool, S. Steele, N. Mangra & D. Gordon. ROM 100073-20849 (juvenile male, 182 mm DW), Demerara River, 6.821667 -58.183778, Mar 2015, M. Kolmann, A. Little, E. Liverpool, S. Steele, N. Mangra & D. Gordon. ROM 103015b-NL10108 (juvenile female, 220 mm DW), Demerara River, 6.543444 -58.243833, Mar 2015, N. M. Kolmann, A. Little, E. Liverpool, S. Steele, N. Mangra & D. Gordon. ROM 103015c-NL10112 (juvenile male, 175 mm DW), Demerara River, 6.543444 -58.243833, Mar 2015, M. Kolmann, A. Little, E. Liverpool, S. Steele, N. Mangra & D. Gordon. ROM 103015d-NL10109 (juvenile female, 190 mm DW), Demerara River, 6.543444 -58.243833, Mar 2015, M. Kolmann, A. Little, E. Liverpool, S. Steele, N. Mangra & D. Gordon. ROM 103015e-NL10113 (juvenile male, 191 mm DW), Demerara River, 6.543444 -58.243833, Mar 2015, M. Kolmann, A. Little, E. Liverpool, S. Steele, N. Mangra & D. Gordon. ROM 100073-20847 (juvenile male, 229 mm DW), Demerara River, Guyana, 6.543444 -58.243833, Mar 2015, M. Kolmann, A. Little, E. Liverpool, S. Steele, N. Mangra & D. Gordon. Río Guanare, Venezuela. ROMT8998/AUM53789 (juvenile male, 128 mm DW), 15km SW of Río Guanare, 8.91411 -69.76110, Mar 2010, N. K. Lujan, M. H. Sabaj, T. Carvalho, D. C. Werneke, K. Roach & V. Meza.

Diagnosis. *Potamotrygon siponinmorok* is distinguished from sympatric congeners, except for polymorphic *P. orbignyi* (see da Silva, 2010), by its coloration consisting of dorsal disk dark brown, medial region with small light brown rosettes joined to form a hexagonal pattern from interorbital region to tail base (*vs*. dark brown background with orange-red ocellated spots irregular in shape, surrounded by broad concentric black rings in *P. boesemani*, dark brown background with light spots about twice orbit size, formed by clusters of ~50 smaller spots in *P. marinae*, black background with tan, beige, golden yellow, or orangish rosettes in *P. schroederi*, and graybrown background with conspicuous tricolored ocelli: central yellow spot, intermediate orange ring, external black ring in *P. motoro*; Fig. 4). *Potamotrygon siponinmorok* is distinguished from *P. orbignyi* by the labial ridges present at the corners of the lower jaw but weakly developed and not distinctly demarcated (*vs*. well-developed labial groove), 28 and 35 upper and lower tooth rows, respectively (*vs*. 35 and 33), teeth blunt and smooth (*vs*. with triangular crowns, slightly monocuspid in males or trapezoidal and tricuspid in females, see da Silva, Carvalho, 2015), lateral line with a bridge connecting the suborbital loop and infraorbital loop (*vs*. bridge absent), hyomadibular cartilage thick with curved ends (*vs*. slender and straight ends), posterior subpleural tubules are absent (*vs*. present), and total number of vertebrae 131 (*vs*. 125).

Potamotrygon siponinmorok is further distinguished from congeners by a dark pigmented crescent-shaped blotch positioned dorsal and posterior to spiracle (*vs*. absent in all sympatric congeners), by its ventral surface tan/beige with the posterior margin of the disk gray (*vs*. black posterior margin in *P. boesemani* and dark gray covering the

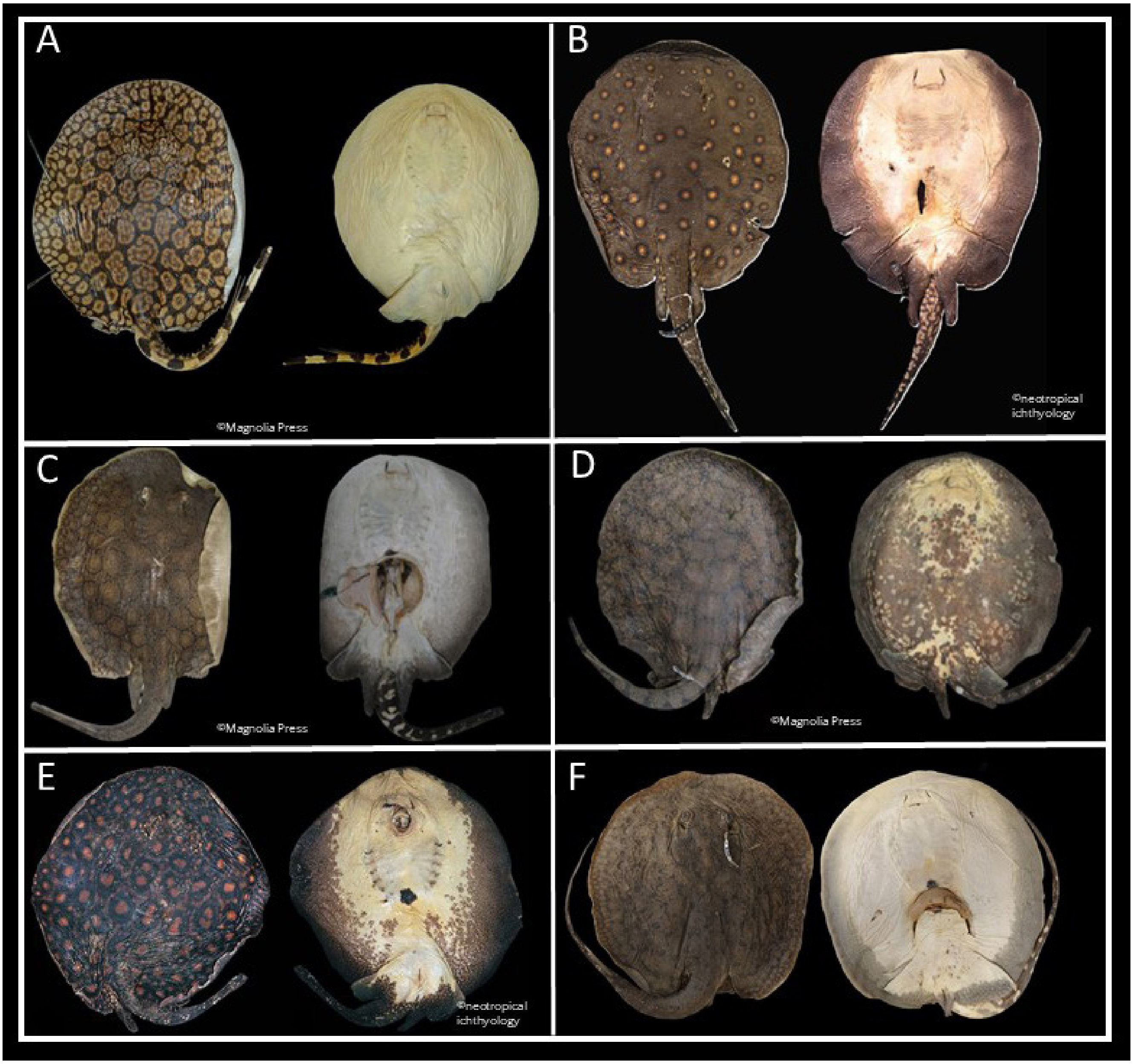

FIGURE 4 | **A–E**, comparative materials. **A.** *Potamotrygon schroederi* (Carvalho *et al*., 2011); **B.** *Potamotrygon motoro* (Loboda, Carvalho, 2013); **C.** *Potamotrygon orbignyi* (da Silva, Carvalho, 2015); **D.** *Potamotrygon marinae* (da Silva, Carvalho, 2015), **E.** *Potamotrygon boesemani* (Rosa *et al*., 2008); **F.** Paratype of *Potamotrygon siponinmorok*. ROM 100073-20848 (juvenile male, 272 mm DW). Insets **A–E** were all reproduced with permission from the copyright holder.

entire surface except the oral cavity in *P. marinae*), by the tail ventral surface displaying beige to light brown bands originating from its the lateral sides, and alternating with dark brown bands (the beige bands remain disconnected while the brown bands connect across the ventral midline) (*vs*. completely black ventral tail in *P. boesemani* and reticulated brown pattern in *P. motoro*), tail relatively long, with a tail length of 120.7% DW (*vs*. 83.9% DW in *P. marinae* and 92% DW in *P. orbignyi*), tail denticles large and arranged in a single row from the base of the tail to the insertion of the stinger (*vs*. no regular order in *P. motoro*; four rows in *P. schroederi*; and no or small spines in *P. orbignyi*), a larger number of denticles concentrated in the center of the dorsal disk (*vs*. denticles covering the entire dorsal disk in *P. motoro*), the tail denticles having a rounded base (*vs*. stellate base in *P. marinae*), and by having a single, long angular cartilage (*vs*. two smaller angular cartilages in *P. motoro* and *P. boesemani*).

Description. External morphology. Disk oval, (slightly) longer than wide (DL 99.6–109.4% DW) (Figs. 2A, B; Tab. 1). Rostrum (anterior margin of disk) not procumbent. Eyes small and oval, approximately 1.5 times smaller than spiracles. Spiracles slightly oblique, with anterior margin close behind eye and posterior end angled toward midline. Head region small, approximately 1/5 of disk length, with interorbital distance ranging from 18.7–21.4% DW and interspiracular distance ranging from 18.1–20.7% DW. Mouth small and slightly undulated (mouth width 6.6–8.9% DW). Internasal distance as wide as mouth width (6.0–8.9% DW). Branchial basket wider than long. Distance between first branchial slits 21.6–26.6% DW and distance between fifth branchial slits 16.8–22.1% DW. Length of the branchial basket 15.9–23.7% DW. Teeth oval-shaped, wider than long. Teeth in an alternate arrangement, not in a straight line, resembling a quincunx. Both upper and lower teeth plates are arranged in an arch. Pelvic fins wide (56.8–59.2% DW), subtriangular, with a pointed and undulated posterior margin. Length of anterior margins of pelvic fins ranging from 17.9–26.4% DW. Claspers are long, cylindrical, and narrow with a rounded tip. Clasper groove long (9.1–13.5% DW), running straight from pelvic fins, and curving medially posterior to dorsal pseudosiphon. Tail width ranging from 10.5–18.3% DW. Tail slightly longer than the disk length (110.0–120.9% DW), it is long and gradually narrows after the insertion of the caudal sting. Caudal sting ranging from 15.4–25.7% DW.

Coloration in alcohol. Dorsal disk background color dark brown (Fig. 3). Patterns on medial dorsal disk made up of small light brown rosettes connected to each other, forming a net-like appearance that extends from interorbital region to base of tail (Fig. 5). Toward disk margin, this pattern becomes more reticulate and individual rosettes no longer distinguishable. Dark pigmented crescent-shaped blotch positioned dorsal and posterior to spiracle (Fig. 6). Ventral color light tan. Marginal region of disk and posterior region of pelvic fin dark gray. Color more intense in adults. Tail with large dark brown bands originating from base of tail, band size reduces moving towards tip of tail; underside of tail beige, similar to coloration of ventral side of disk. Moving towards tip of tail, color of dark brown bands replaced by beige coloration, very tip of the tail completely dark brown.

Dermal denticles. Dermal denticles distributed across dorsal disk and tail, with different morphologies. The center of disk has higher concentration of star shaped denticles, with a maximum diameter of 1.2 mm. Margins of disk with pointed dermal denticles with rounded base. Posterior portion of disk with denticles of posteriorly oriented cusps, larger than anterior denticles. Anterior margin with pointed denticles with a single cusp (Fig. 7A) and have higher number of denticles in comparison to other regions of disk. Tail region with thorn-line, posteriorly oriented, single cusp denticles, with broad and rounded basal plate. Caudal denticles organized in single row, extending

FIGURE 5 | Rosette-like pattern on the dorsal surface of *Potamotrygon siponinmorok*. Paratype, ROM 100073-20848 (juvenile male, 272 mm DW).

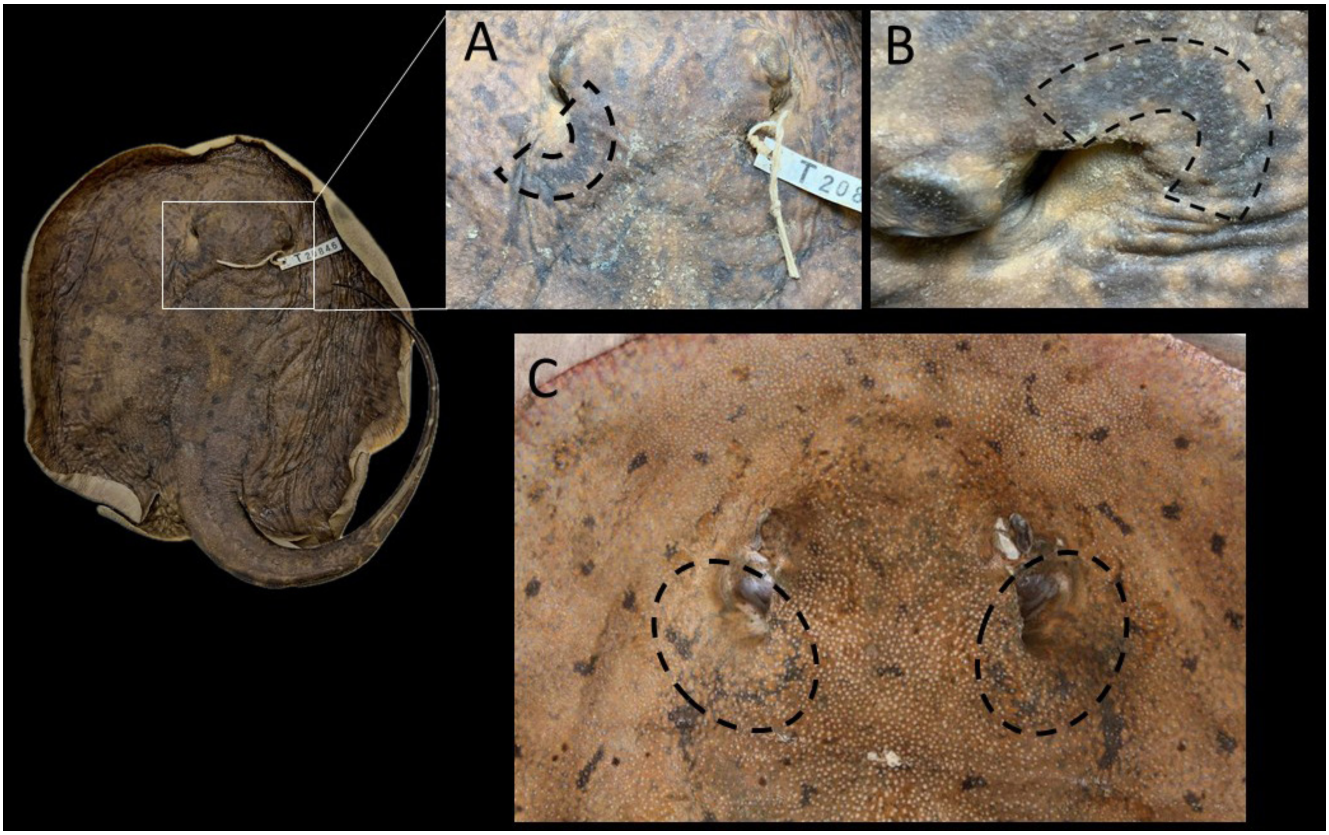

FIGURE 6 | A dark pigmented crescent-shaped blotch positioned dorsal and posterior to the spiracle opening **A.** Dorsal view; **B.** Lateral view of *Potamotrygon siponinmorok*, Holotype, CSBD F3260 (juvenile male, 224 mm DW); and **C.** Dorsal view of *P. siponinmorok*. Paratype, ROM 100992-20688 (adult female, 353 mm DW).

from base of tail to insertion of caudal sting (N = 17 in holotype CSBD F3620). Smaller single cusp denticles, irregularly organized on sides of tail (Fig. 7D).

Ventral lateral line system. The hyomandibular canal (HYC) originates at anteriormost region of disk, curving to margin of disk. The anteriormost region of hyomandibular component (HYC) connected to multiple short and straight anterior subpleural tubules (AST). Subpleural component of hyomandibular canal (SPC) slightly undulated, projecting posteromedially along margin of disk. Subpleural component (SPC) gradually curves inwards, towards insertion of pelvic fin and abruptly curves anteriorly, forming the subpleural loop (SPL). Posterior subpleural tubules absent. Jugular component of hyomandibular canal (JCH) projects anteriorly and obliquely, bordering external margin of branchial basket. Above first gill slits, jugular canal (JUG) extends medially, in an approximate 75° angle, presenting numerous undulations and forming posterior jugular loop (PJL). Extending from posterior jugular loop (PJL), a short nasal canal (NAS), which projects medially, running towards oral cavity. Extending laterally from base of nasal canal (NAS), is formation of infraorbital loop (IOL). Hyomandibular canal then extends to infraorbital loop (IOL) anteriorly and continues until it reconnects with hyomandibular canal (HYC) on anterior most point, forming suborbital loop (SOL) (Fig. 8).

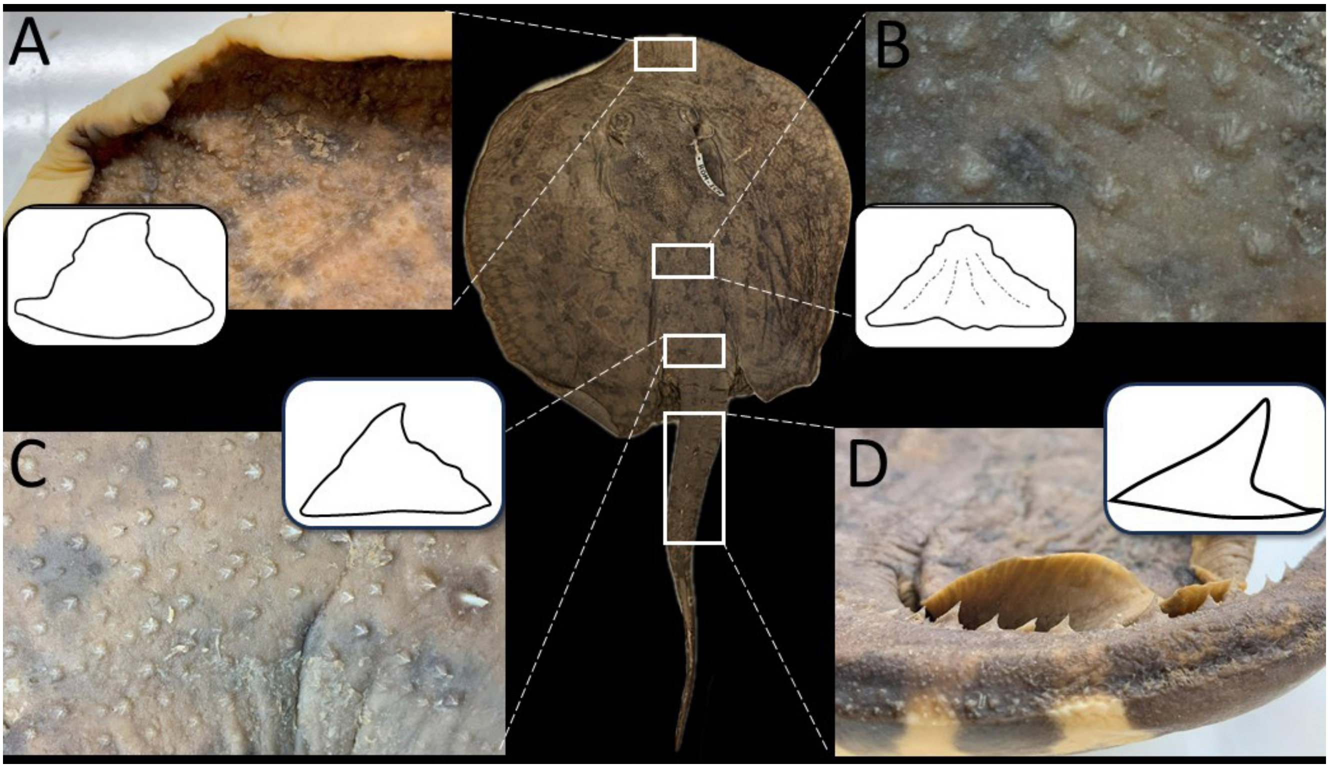

FIGURE 7 | Dermal denticles on the disk of *Potamotrygon siponinmorok*. Holotype, CSBD F3620 (juvenile male, 224 mm DW).

Jaws and teeth. Teeth are ovoid, blunted, and smooth, and are arranged in a quincunx (five teeth with four forming the corners of a square and the fifth at its center) pattern (observation is seen more predominantly at the center of the tooth plate). Both jaws have teeth, with medial and lateral teeth identical in size; teeth of medial rows with more developed cusps than lateral teeth (Fig. 9B). Upper tooth row of teeth in holotype is 28 and lower tooth row is 35. Rows of teeth count were done following Rosa (1985). Seven buccal papillae present, five anterior and two posterior (Fig. 9B). Three of anterior papillae centrally positioned, one anterior and two posterior; other two anterior papillae laterally set, on either side of inner buccal cavity (Fig. 9B). Labial ridges are smaller in comparison to other congeners (Fig. 9A).

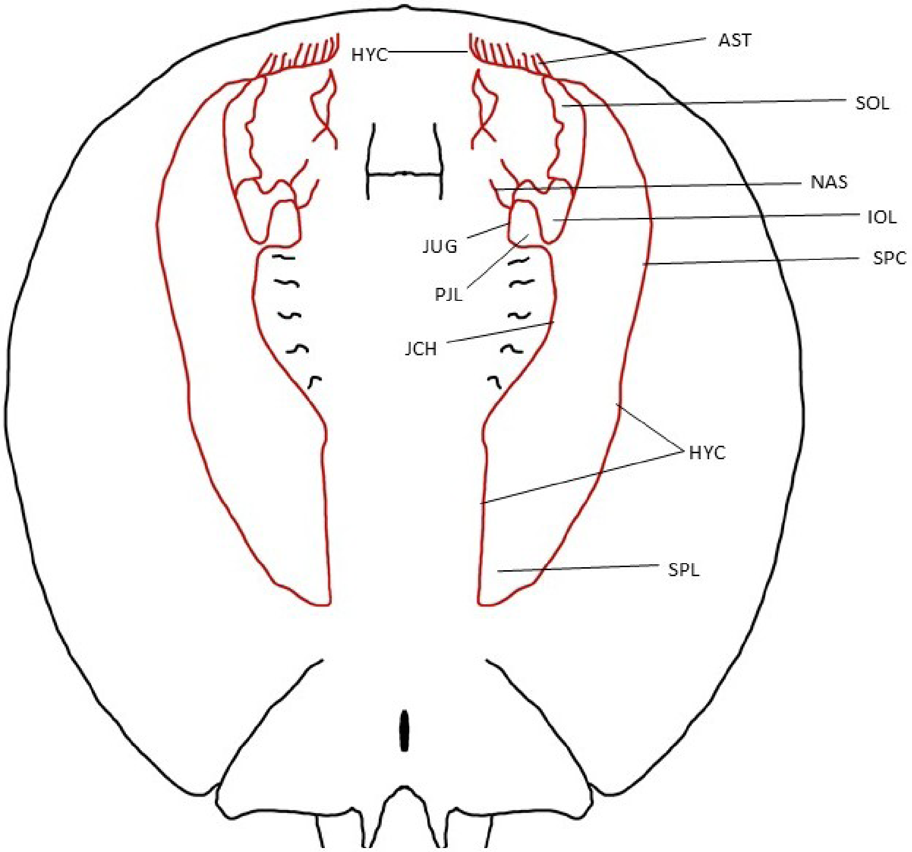

FIGURE 8 | Lateral line system of *Potamotrygon siponinmorok*. Paratype, ROM 100073-20848 (juvenile male, 272 mm DW). Abbreviations: AST, anterior sub pleural tubules; HYC, hyomandibular canal; IOL, infraorbital loop; JCH, jugular component of the hyomandibular canal; JUG, jugular canal; NAS, nasal canal; PJL, posterior jugular loop; SOL, suborbital loop; SPC, subpleural component of the hyomandibular canal; SPL, subpleural loop (adapted from Fontenelle *et al*., 2014).

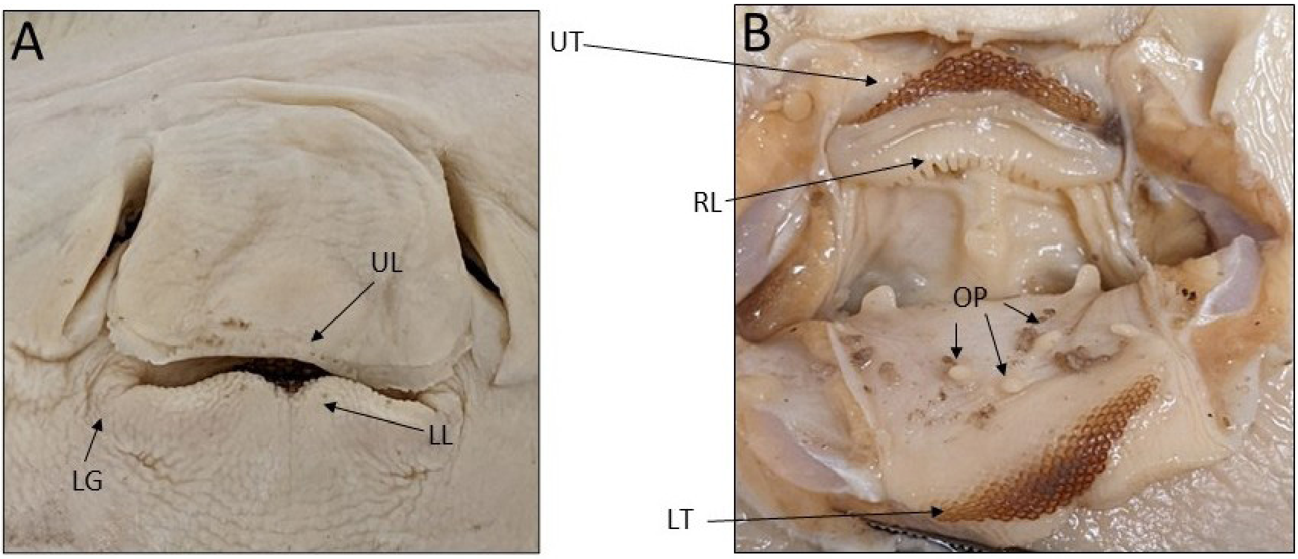

FIGURE 9 | Mouth, teeth and oral papillae of holotype of *Potamotrygon siponinmorok*. Holotype, CSBD F3620 (juvenile male, 224 mm DW). **A.** Detail of mouth; **B.** Detail of open mouth with upper and lower jaw dentition and oral papillae. Abbreviations: UT, upper teeth; LT, lower teeth; UL, upper lip; LL, lower lip; LG, lip groove; RL, rostrum labium; OP, oral papillae.

Claspers. Claspers are conical and slightly tapered distally. Clasper groove (CG), apopyle (AP), hypopyle (HY) and dorsal pseudosiphon (PS) and ventral pseudosiphon (VPS) are located at dorsal face of clasper. Clasper groove originates at distal margin of pelvic fin (apopyle) and extends obliquely from internal to external margin of claspers. Dorsal pseudosiphon is elliptical and obliquely oriented in relation to midline and is situated adjacent to internal margin of clasper. Hypopyle (HY) gradually curves as it extends distally to tip of clasper (Fig. 10).

Skeleton description. Meristic counts of vertebrae and pectoral and pelvic radials are shown in Tab 1. In dorsal view, nasal capsules (NC) almost oval, separated by a very small internasal septum (IS), anteriorly surrounded by first segment of propterygium and laterally connected with propterygium (PRO) through long triangular antorbital cartilage (ANT). Roof of neurocranium with a large fontanelle (larger anteriorly and narrows posteriorly), from nasal capsules to posterior part of orbital region. Fontanelle divided into two components: an anterior, rounded and broad precerebral component (PCF), and a posterior, long, narrow frontoparietal component (FPF) (Fig. 11A). Mandibular arch laterally extended, with long and proximally arched palatoquadrate (PQ) and which articulates with the Meckel's cartilage (MC). Meckel's cartilage with a pronounced arch in its proximal portion where it articulates with palatoquadrate. MC with a knob like lateral process (LP) (Fig. 11B). Hyomandibula (HYO) long and wide with its distal portion anteriorly curved (Fig. 11A). Anterior angular cartilage wide, crescent-shaped, and connecting slightly below lateral process anteriorly, with lateral head connecting to hyomandibular process (Fig. 11C). Anterior synarcual condyle linking to posterior neurocranium robust and strongly interdigitating with neurocranium. Coracoid bar (COB) dorsoventrally flattened, anterodorsally straight and laterally expanded. Three condyles contact the basal elements of the pectoral fin.

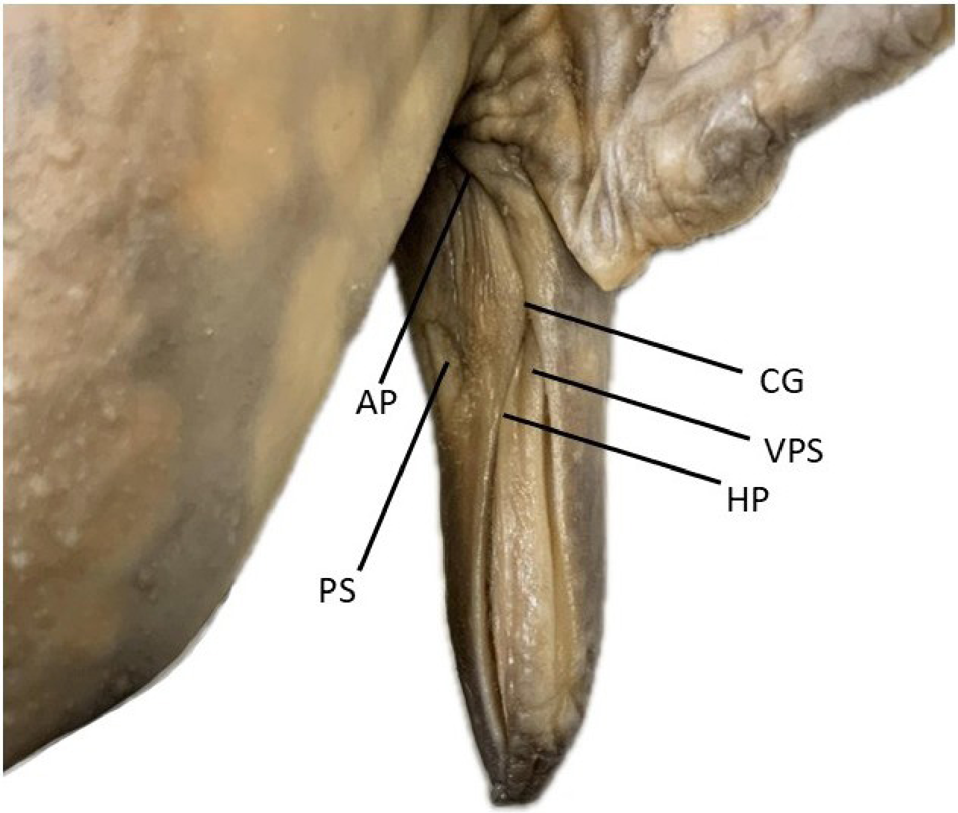

FIGURE 10 | Dorsal view of the claspers of *Potamotrygon siponinmorok*. Paratype, ROM 100073-20848 (juvenile male, 272 mm DW). AG, apopyle; CG, clasper groove; HG, hypopyle; PS, dorsal pseudosiphon; VPS, ventral pseudosiphon.

Procondyle (PC), widest pectoral condyle, slender and long, vertically disposed at anterior lateral face of scapula. Mesocondyle (MSC) oval and horizontally arranged. Metacondyle (MTC), smallest condyle, nearly ovoid and situated on lateral aspect of posterior scapula (Fig. 11D). Puboischiadic bar (PIB) slightly arched, with anterior margin convex and posterior margin concave (Figs. 11A, E).

Morphometric analysis. PCA analysis recovered that individuals of *P. siponinmorok* formed a cluster distinct from sympatric *Potamotrygon* spp. (Fig. 12). Principal Component Analysis (PCA) of nine *Potamotrygon* species revealed that the first four principal components explained 51.29% of the total morphological variation (Figs. 12–13). PC1 accounted for the largest proportion of variance (17.16%), followed by PC2 (12.58%) and PC3 (11.20%). PC1 was primarily associated with disk length and oral width, while PC2 was influenced by the distance between the first gill slit and outer clasper length. PC3 captured variation in preorbital distance, pelvic fin width, caudal sting width, and interorbital distance. The PCA plot indicated that *P. siponinmorok* has a greater distance from the cloaca to the caudal sting origin compared to other species (Figs. 12–13). *Potamotrygon scobina* grouped closely with *P. siponinmorok* but exhibited a comparatively greater prenasal distance. In contrast to *P. siponinmorok*, both *P. marinae*

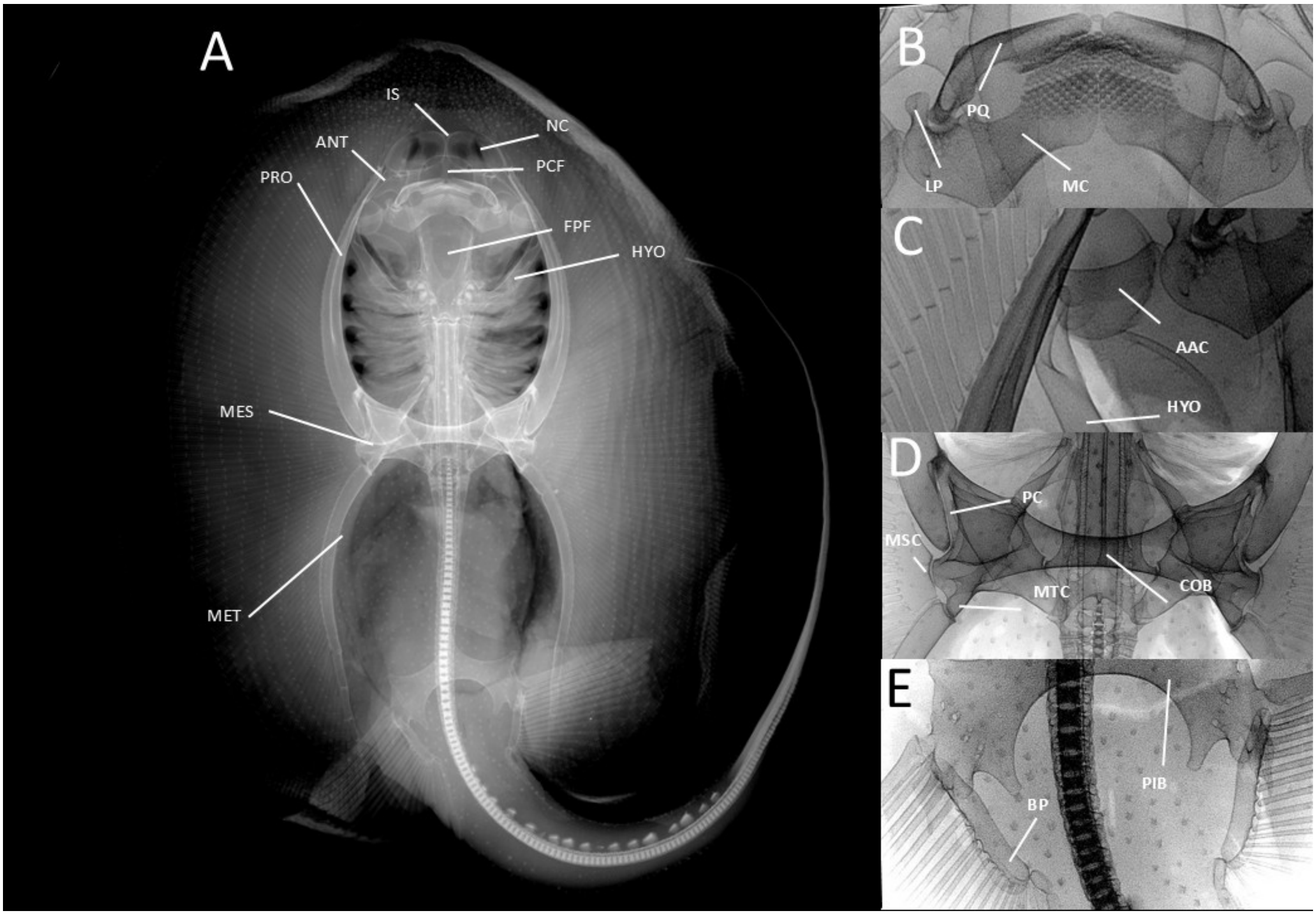

FIGURE 11 | Skeletal anatomy (from radiographs) of holotype of *Potamotrygon siponinmorok*. CSBD F3620 (juvenile male, 224 mm DW). **A.** Entire skeleton; Abbreviations: HYO: hyomandibular process; PCF: precerebral component; FPF: frontoparietal component; ANT: antorbital cartilage; NC: nasal capsule; IS: internasal septum; MES: mesopterygium; MET: metapterygium; PRO: propterygium; **B.** Detail of jaw region; Abbreviations: LP: lateral process; MC: Meckel's Cartilage; PQ: palatoquadrate cartilage. **C.** Detail of angular cartilages; Abbreviations: AAC: anterior angular cartilage; HYO: hyomandibular cartilage; **D.** Detail of pectoral girdle; Abbreviations: COB: coracoid bar; MSC: mesocondyle; MTC: metacondyle; PC: procondyle; **E.** Detail of pelvic girdle; Abbreviations: BP: basipterygium; PIB: puboischiadic bar.

and *P. adamastor* exhibited clear morphological distinctions, with *P. marinae* characterized by increased tail width and *P. adamastor* by greater oral width. *Potamotrygon siponinmorok* formed a tight cluster within one quadrant of the plot, a pattern similarly observed for *P. marinae*. In comparison, *P. orbignyi*, *P. adamastor*, *P. scobina*, and *P. boesemani* were more widely scattered across the plot, suggesting higher morphological variability. The two specimens of *P. schroederi* were positioned at opposite ends of the PC1 axis, indicating substantial intraspecific variation along this principal component.

The PCA plot with the five species that have similar coloration (*P. marinae*, *P. siponinmorok*, *Potamotrygon* sp. (Mahaica), *Potamotrygon* sp. and *P. orbignyi* (Fig. 13) showed that the first three PCs explained 46.83% of the variation. PC1 (17.94%) was strongly associated with the distance between the first gill slit, eye length, and oral width. PC2 (16.23%) contrasted clasper size and structure with total length and cloacal features. PC3 (12.66%) distinguished individuals based on pelvic fin width, the distance

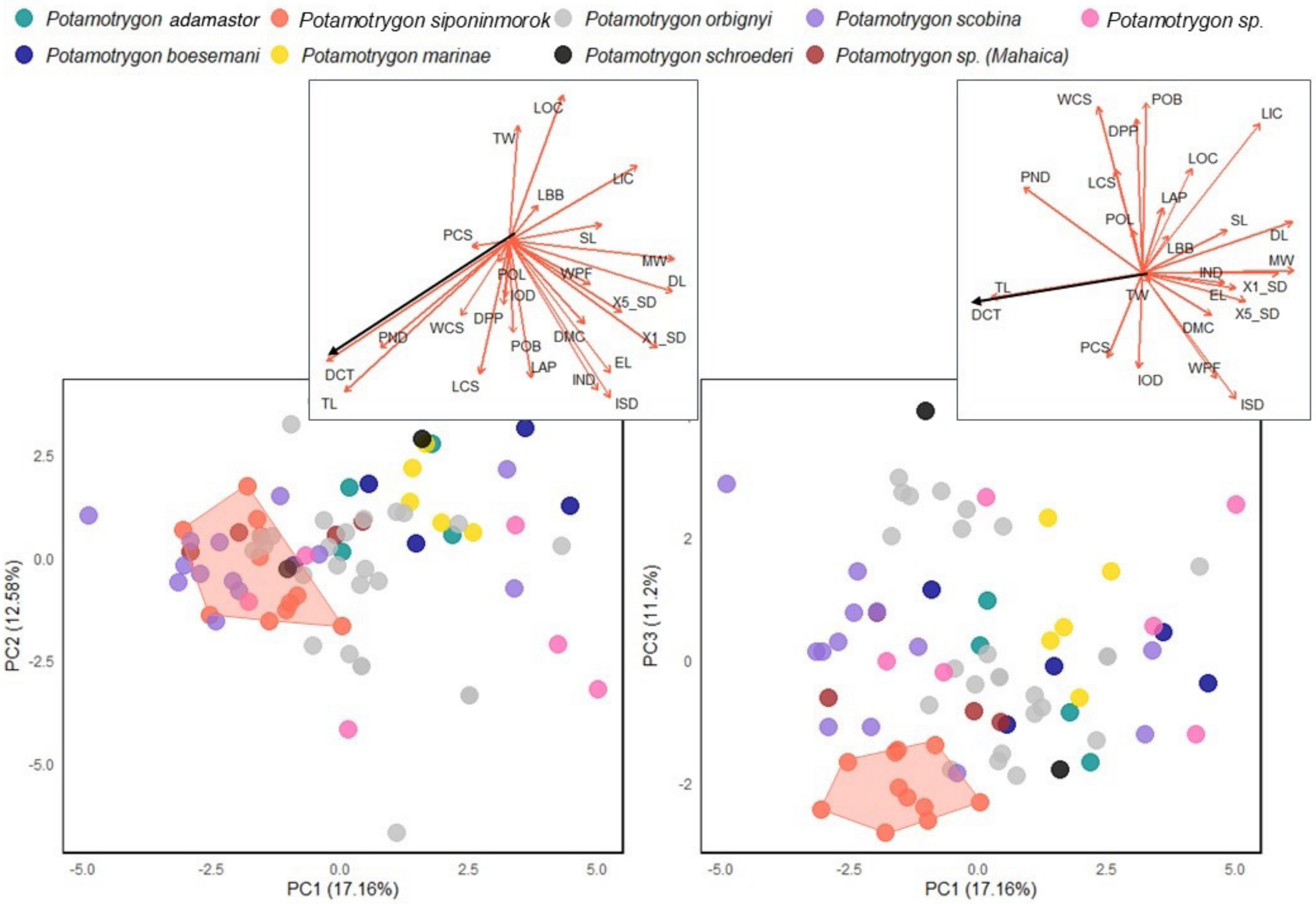

FIGURE 12 | Principal component analysis (PCA) of morphometric variables for nine species of *Potamotrygon*. The first three Principal Components (PCs) are shown, explaining 17.16%, 12.58%, and 11.20% of the variance, respectively. Morphospace of *P. siponinmorok* is indicated by the orange shaded region. The distance between the cloaca and tail tip (DCT) is the distinguishing morphometry between *P. orbignyi* and *P. siponinmorok* and is indicated by a black arrow in the upper right-hand corner of the plot. See methods for abbreviations.

from the underside of the pectoral to the posterior pelvic margin, and caudal sting length. In this analysis, *P. siponinmorok* again formed a distinct and cohesive cluster, exhibiting strong loadings on traits such as cloaca to caudal sting origin, cloaca to tail tip, and total length, consistent with the patterns observed in the broader nine-species PCA. Similarly, individuals of *P. marinae* clustered closely together. In contrast, *P. orbignyi*, *Potamotrygon* sp. (Mahaica), and *Potamotrygon* sp. appeared more dispersed across the plot, indicating greater morphological variation within these taxa.

Molecular analysis. *Potamotrygon siponinmorok* is placed within a distinct clade (Clade A, Fig. 14) with high support (bootstrap 100, aLRT SH-like 100) within the *P. orbignyi* species complex (Fontenelle *et al*., 2021b). *Potamotrygon siponinmorok* individuals form a monophyletic clade (bootstrap 96.4, aLRT SH-like 97). Other members of Clade A include individuals of *P. orbignyi* and *P. schroederi*, and a lineage representing *P. marinae*. The *P. siponinmorok* individuals are 0.8% genetically diverged from the *P. schroederi* individuals (RN11-24, RN05-01 and AUM54482). Given the complex species

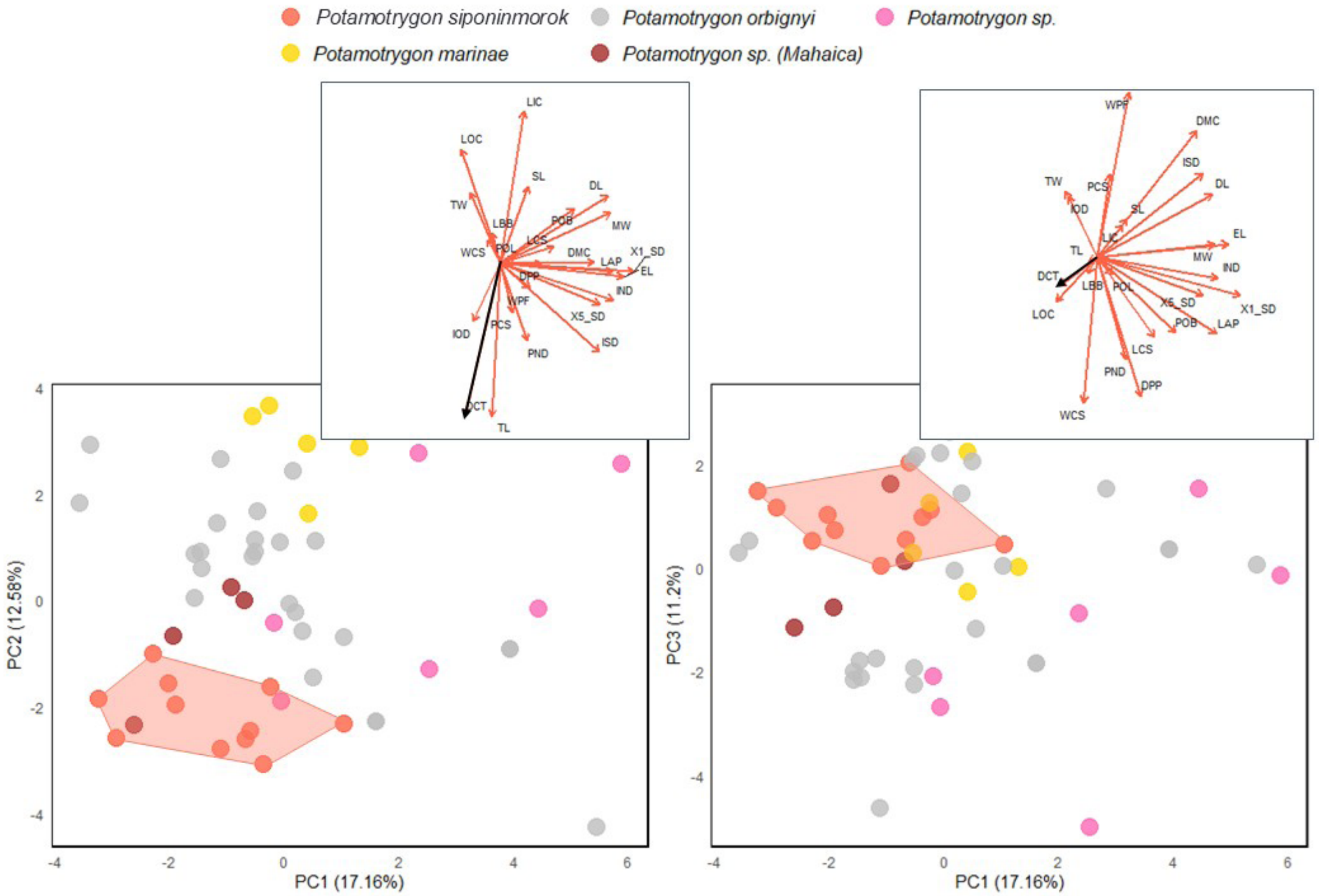

FIGURE 13 | Principal component analysis (PCA) of morphometric variables for six species of *Potamotrygon* that show similar morphology. *Potamotrygon boesemani*, *P. scobina*, and *P. adamastor* from Fig. 12 were excluded from this plot, as their distinct color patterns and morphology allow for easy species identification when compared to the six species plotted here. The first three Principal Components (PCs) are presented, accounting for 17.94%, 16.23%, and 12.66% of the variance, respectively. Morphospace of *P. siponinmorok* are indicated by the orange shaded region. The distance between the cloaca and tail tip (DCT) is the distinguishing morphometric between *P. orbignyi* and *P. siponinmorok* and is indicated by a black arrow in the upper right-hand corner of the plot. See methods for abbreviations.

boundaries frequently observed within *Potamotrygon*, such low divergence may still reflect species-level distinctiveness (see Discussion). *Potamotrygon siponinmorok* and *P. marinae* are genetically distinct with a divergence of 3.6%. The closest relatives of Clade A are *P. boesemani* individuals, which are 2.4% genetically distant from *P. siponinmorok*.

Geographical distribution. Currently, *Potamotrygon siponinmorok* is known from the Demerara River, Region 4 (Demerara-Mahaica), Guyana near the capital Georgetown and río Guanare, Orinoco drainage, Venezuela (Fig. 1; Tab. **S1**).

Conservation status. *Potamotrygon siponinmorok* is currently known from only two drainages: the Demerara River in Guyana (based on several specimens) and the río Guanare in Venezuela (based on a single specimen), suggesting a species with restricted distribution and a small number of known locations. Although these areas are under considerable threat of anthropogenic activities, like exploratory fishing, boat/shop traffic,

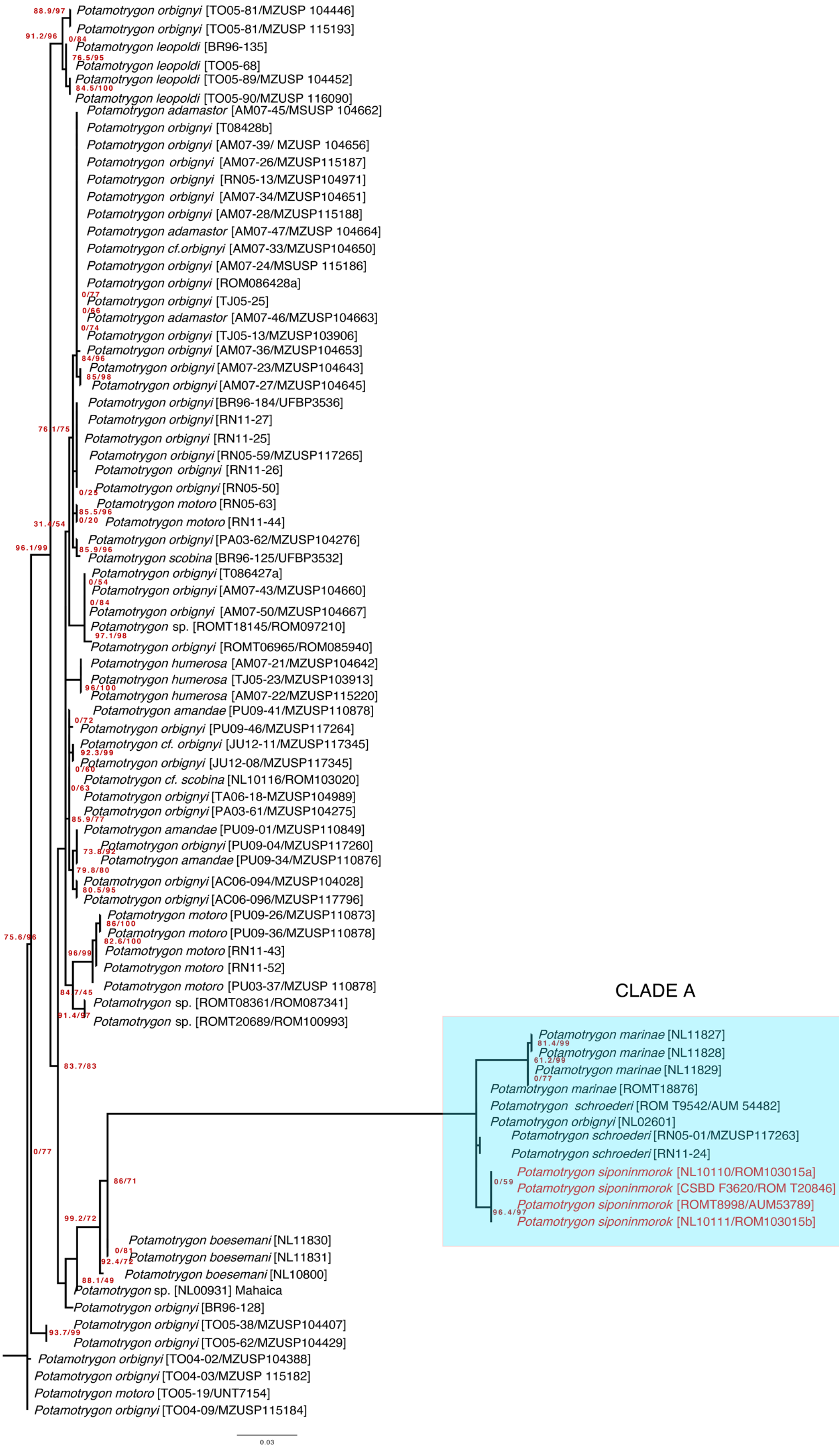

FIGURE 14 | Phylogenetic relationships of Potamotrygonidae based exclusively on Cytochrome c oxidase subunit I (COX1), with clade A.

illegal waste disposal, and chemical runoff from agricultural practices (D. Gordon, 2015, pers. comm.), their impact on *P. siponinmorok* populations and habitat quality remain unknown. Given the absence of data on population size and trends (IUCN Criteria A and C) and the lack of quantitative analyses pertaining to extinction risk (Criterion E), we recommend that *Potamotrygon siponinmorok* be classified as Data Deficient (DD), following current IUCN Red List criteria (IUCN, 2024). Further sampling of western Guyana and eastern Venezuela drainages are necessary for proper assessment of *P. siponinmorok* area of occupancy (AOO), extent of occurrence (EOO), population demography and trends in order to evaluate the degree of habitat degradation needed for a robust assessment.

Ecological notes. The authors report that in the Demerara estuary, adult *Potamotrygon siponinmorok* occasionally, co-occur with obligate marine stingrays such as *Hypanus geijskesi* (Boeseman, 1948) and *H. guttatus* (Bloch & Schneider, 1801) after periods of heavy freshwater outflow. In contrast, smaller juveniles of *P. siponinmorok* are observed several miles upstream of the estuary. Individuals of this species collected from the Demerara River are subject to tidal influence (Narayan, 2006), enabling movement throughout the estuarine regions. Preliminary observations of stomach contents indicate that *P. siponinmorok* primarily preys on aquatic insect larvae, decapod crustaceans, and, less frequently, small fishes. The species predominantly inhabits environments characterized by sandy substrates with minor mud deposits. The riverbanks are populated with dense vegetation, primarily consisting of mangrove trees. The water body is turbid and significantly influenced by tidal fluctuations (Narayan, 2006). Despite their incidental capture during fishing, stingrays are not targeted for consumption; individuals are typically released back into the water unharmed. However, in some instances, the tail with the venomous stings are removed prior to release.

Etymology. The new species is named to acknowledge the Akawaio people, the Indigenous community historically occupying coastal Guyana, near where the holotype was collected. The species name derives from the Akawaio phrase *si ponin moro*, meaning the "fish that stings." The "si" is pronounced like "chee" and the "moro" like "moor-okh" for English and Creole speakers.

Remarks. *Potamotrygon roulini* was collected from the same basin in Colombia as one of our paratypes. However, we were unable to compare *P. siponinmorok* with *P. roulini* because no diagnosis or standard morphometric data were provided in the original description of *P. roulini*. Furthermore, the taxonomic status of *P. roulini* remains uncertain, as its validity has been called into question (da Silva *et al*., 2021).

Comparative material examined. *Potamotrygon boesemani*. The same listed at Rosa *et al.* (2008), with the addition of: USNM 225574, 377 mm DW, Matapi Creek, *ca.* 1 km from Corantijn River, Nickerie District, Surinam, 05°00'N 57°16'W, 9 Sep 1980, R. Vari *et al.* USNM 225216, female, 153 mm DW, stream about 0.5 km inland of Camp Mataway, Nickerie District, Surinam, 04°48'N 57°43'W, 12 Sep 1980, R. Vari *et al.* USNM 225575, 250 mm DW, Corantijn River at km 180, Nickerie District, Surinam, 05°08'N 57°18'W, 8 Sep 1980, R. Vari *et al.* USNM 388849, 413 mm DW, 427 mm DW, Matapi Creek, *ca.* 1 km from Corantijn River, Nickerie District, Surinam, 05°00'N 57°16'W, 9 Sep 1980, R. Vari *et al. Potamotrygon marinae*. The same listed at Deynat (2006), with the addition of: MNHN 2006-0750, 238 mm DW, Maroni, grand Inini, 1997, Le Bail, Keith, Jégu *et al*. MNHN 1998-1811, 160 mm DW, Maroni, Tampoc, 1998, Le Bail & Keith. MNHN 2003-0020, 153 mm DW, Antecume Pata, Maroni River, Litany, 2002, Fermon, Ksas, Commergnat *et al*. MNHN 1998-2006, 412 mm DW, Maroni, Grand Inini, 1997, Le Bail, Keith, Jégu *et al*. *Potamotrygon motoro*. The same listed at Loboda, Carvalho (2013), with the addition of: NMW 77987, 201 mm DW, rio Cuiabá, district of Cuiabá, State of Mato Grosso, Brazil, J. Natterer. NMW 78613, 344 mm DW, rio Cuiabá, district of Cuiabá, State of Mato Grosso, Brazil, Aug 1824, J. Natterer. ZMB 4662, 183 mm DW, rio Cuiabá, district of Cuiabá, State of Mato Grosso, Brazil, J. Natterer. *Potamotrygon orbignyi*. The same listed at da Silva, Carvalho (2015), with the addition of: MNHN 2333, 465 mm TL, 216 mm DL, 275 mm DW, Tocantins, Tocantins River, Brazil. MZUSP TO04.01, 328 mm DL, Tocantins, Biura Lagoon, Palmas River, São Pedro farm, Tocantins-Araguaia basin, Amazon River basin, Brazil. MZUSP TO04.04, 285 mm DL, Tocantins, Biura Lagoon, Palmas River, São Pedro farm, Tocantins-Araguaia basin, Amazon River basin, Brazil. MZUSP TO04.09, 230 mm DL, Tocantins, Biura Lagoon, Palmas River, São Pedro farm, Tocantins-Araguaia basin, Amazon River basin, Brazil. *Potamotrygon schroederi*. The same listed at Carvalho *et al*. (2011), with the addition of: MZUSP 108453, (689 mm TL, 444 mm DL, 409 mm DW, rio Negro, Brazil. MZUSP 108452, 741 mm TL, 444 mm DL, 395 mm DW, rio Negro, Brazil. MZUSP 108445, 501 mm TL, 320 mm DL, 290 mm DW, rio Negro, Brazil. MZUSP 108455, 319 mm TL, 202 mm DL, 188 mm DW, rio Negro, Brazil. AUM 44507, adult male, 780 mm TL. ANSP 191999, adult female, 605 mm TL.

DISCUSSION

Potamotrygon siponinmorok exhibits a unique combination of morphological traits and is genetically distinct from other congeners occurring in the same river system, or regional river systems, confirming its status as a distinct species. Based on meristic and morphometric characters, *P. siponinmorok* consistently clustered apart from other species in our PCA morphospaces, highlighting its morphological distinctiveness from congenerics. A unique feature that distinguishes *P. siponinmorok* from congeners such as *P. orbignyi*, *P. boesemani*, and *P. marinae*, is the presence of a black crescent-shaped blotch positioned posterior and dorsal to the spiracle (Fig. 6). Additionally, the dorsal side of *P. siponinmorok* lacks the ocellated patterns as seen in *P. boesemani* and *P. motoro* or the yellow rosette pattern of *P. schroederi*. The dorsal pattern and coloration of *P. siponinmorok* most closely resembles that of *P. marinae* and *P. orbignyi*; however, based on our morphometric data and illustrations by the PCA plots (Figs. 12–13), the length of the tail (specifically, from the cloaca to the tail tip) in *P. siponinmorok* is longer than both of aforementioned species. Additionally, *P. siponinmorok* teeth are smooth and ovoid while *P. orbignyi* teeth are very small, with triangular crowns, slightly monocuspid in males and trapezoidal, tricuspid in females (da Silva, Carvalho, 2015). Additionally, the number of upper tooth rows is fewer in *P. siponinmorok* (28 *vs*. 35) than in *P. orbignyi*. Regarding the skeleton, *P. siponinmorok* has a thick hyomandibular cartilages with slightly curved ends (compared to slenderer hyomandibulae with straight edges in *P. orbignyi*). *Potamotrygon siponinmorok* is morphologically and genetically similar to *P. orbignyi* and represents the most recently recognized species to be formally separated from the *P. orbignyi* species complex.

Many species of *Potamotrygon* exhibit extensive morphological variation and phenotypic plasticity, leading to challenges in accurate identification and classification (Fontenelle *et al*., 2021b). For example, Rincon Filho (2006), made notations of the various colorations and patterns observed in *P. orbignyi* species complex, and noted six patterns (*e.g.*, reticulated, dotted, spotted, ocellated, vermiculate and rosetted), all of which are also observed in other species of *Potamotrygon*. Therefore, the coloration and pattern comparison between *P. siponinmorok* and *P. orbignyi* can be difficult to distinguish as the latter is polymorphic and geographically widespread (see da Silva, 2010).

Potamotrygon orbignyi exhibits considerable variation in coloration and morphology (da Silva, Carvalho, 2015) and is frequently found in non-monophyletic arrangements with *P. schroederi* (Fernández-Yépez, 1958), *P. marinae* (Deynat, 2006), *P. adamastor* (Fontenelle, Carvalho, 2017), *P. garmani* (Fontenelle, Carvalho, 2017), *P. henlei* (Castelnau, 1855), and more recently, *P. siponinmorok*. Specimens of *P. orbignyi* often show a greater affinity with other species of *Potamotrygon* in the same river basin (Toffoli *et al.*, 2008; Fontenelle *et al.*, 2021a). *Potamotrygon orbignyi* is among the most widely distributed species of *Potamotrygon* in the Neotropics, occurring throughout the upper, middle, and lower Amazon basin as well as in the Orinoco and Guiana Shield drainages (da Silva, Carvalho, 2015). In contrast, *P. siponinmorok*, at least from what is currently known, is restricted to only two basins in Northern South America: the Demerara River (Guyana) and río Guanare (Venezuela). In this way, *P. siponinmorok* is akin to other *Potamotrygon* species with narrow distribution ranges; for example, *P. marinae* (endemic to only several drainages in Guyana and Suriname; Taphorn *et al.*, 2022), *P. boesemani* (endemic to the Corantijne River, Suriname; Deynat, 2006), and *P. garmani* and *P. henlei* (both endemic to the Tocantins-Araguaia River; Fontenelle *et al.*, 2021a).

The disjunct distribution of individuals of *P. siponinmorok* in our study, *i.e.*, Guyana but with one specimen known from the río Guanare (Venezuela), presents a biogeographical conundrum. There are two potential biogeographical explanations for the presence of *P. siponinmorok* in these regions, either (1) inland dispersal via interconnected river corridors, such as the Casiquiare-Negro-Rupununi rivers, or (2) coastal dispersal through freshwater plumes or during periods of lower sea level. The Casiquiare River connects the Orinoco basin to the río Negro in southwest Venezuela and may act as both a filter and corridor for faunal dispersal between Orinoco and Amazonian faunas (Winemiller *et al.*, 2008). Likewise, the Rupununi Portal is a seasonal savanna floodplain in Guyana that connects the Rupununi River to the Upper Branco River, and by extension, the río Negro (Souza *et al.*, 2012, 2020). The río Guanare drains into the río Apure, and by extension the Orinoco and Casiquiare, providing a potential contiguous corridor for dispersal by these rays into Guyana's waterways, assuming they can cross deeper channels. The biogeographical influence of these corridors have been hypothesized to explain the distribution of different groups of fish inhabiting this region, including needlefish (*e.g.*, Lovejoy, Araújo, 2000), cichlids (*e.g.*, Willis *et al.*, 2010), catfishes (*e.g.*, Souza *et al.*, 2012, 2020), characins (*e.g.*, Turner *et al.*, 2004) and stingrays (*e.g.*, Fontenelle *et al.*, 2021a). However, if a contiguous Guanare-Casiquiare-Demerara corridor is present one might expect the *P. siponinmorok* clade to be recovered phylogenetically close to other lineages found in the areas that form these corridors. The lack of this evidence based on our COX1 dataset (Fig. 14) weakens the assumption that *P. siponinmorok* would be continuously distributed from Guyana to Venezuela through this route. Additional sampling is necessary between the current known occurrence and other drainages inland, to corroborate any biogeographical corridors (*e.g.*, proto-Berbice, Rupununi portal – Lujan, Armbruster, 2011; Souza *et al.*, 2012).

Alternatively, the disjunct distribution of *P. siponinmorok* could be more consistent with a hypothesis including coastal dispersal, facilitated by lower sea-level periods or using freshwater plumes as seasonal corridors (Lemopoulos, Covain, 2018). Such coastal exchanges are known in other parts of the Guianas and hypothesized to explain the occurrence of widespread taxa like *Hoplias malabaricus* (Bloch, 1794), *Astyanax bimaculatus* (Linnaeus, 1758), and *Curimata cyprinoides* (Linnaeus, 1766) across multiple coastal streams in French Guiana (Le Bail *et al*., 2012). Additionally, large adult specimens of *P. siponinmorok* were observed co-occurring with marine rays (*e.g*., *Hypanus geijskesi*) in the Demerara estuary, suggesting that this species, or at least adults, exhibits greater tolerance to euryhaline conditions than previously recognized. Guyana's immediate coastal shelf could have been more exposed during glacial periods (Lujan, Armbruster, 2011; Lemopoulos, Covain, 2019), when sea-levels may have been quite lower than they were today, making dispersal among coastal rivers easier for freshwater lineages. The fish faunas of the western reaches of Guyana are poorly known (Taphorn *et al*., 2022), compared to the rest of the country, in part due to tensions at the Venezuelan border. We suggest that *P. siponinmorok* may be present in other coastal Guiana Shield drainages in eastern Venezuela (*e.g*., río Arature, río Imataca) and western Guyana (*e.g*., Barima-Waini, Pomeroon), which highlights the need to survey these rivers more thoroughly.

This description of *P. siponinmorok* suggests that our current understanding of species richness in the Guiana Shield is far from complete and may harbor additional cryptic species. These discoveries also have conservation implications, as many freshwater rays are vulnerable due to habitat degradation (Barbosa *et al*., 2025) and unnamed species may go extinct before they are even documented (Alofs *et al*., 2014).

ACKNOWLEDGMENTS

We thank the following volunteers, curators, collection managers, and students for their help on this project: Sophia Putman (University of Michigan) for help with morphometric data collection. Randy Singer and Hernán López-Fernández for help with comparative material at University of Michigan Museum of Zoology. Erling Holm, Don Stacey, Nathan Lujan, Mary Burridge, Kathy Wang, and John Furlone for help with the x-ray of types and comparative material at the Royal Ontario Museum. Diego Elias, Lesley de Souza and Sophie Picq from Chicago Field Museum for help and insight on phylogenetic analysis. Jonathan Armbruster, David Werneke, Emmy Delekta, and Jack Rosen were instrumental in transporting larger stingray specimens. Nevile Mangra and Danny Gordon for help with specimen collection in Guyana. Fernando Marques for providing samples, photos and comments on the phylogeny. We thank Rita Hunter, Katheleen Hunter, and Camille Hunter for help with English to Akawaio translation. We thank the two reviewers for their thoughtful and constructive comments, which greatly improved this manuscript. We are also grateful to Ernesha Fernando (IUCN) for her assistance in assigning a conservation status to the new species.

REFERENCES

- **Alofs KM, Liverpool EA, Taphorn DC, Bernard CR, López-Fernández H.** Mind the (information) gap: the importance of exploration and discovery for assessing conservation priorities for freshwater fish. Divers Distrib. 2014; 20(1):107–13. https://doi.org/10.1111/ddi.12127
- **de Aquino JB, Melo LF, Rodrigues RF, Melo APF, Morais-Pinto L, Rici REG.** Morphological aspects of the digestive system in freshwater stingray (*Potamotrygon amandae* - Loboda and Carvalho, 2013): Myliobatiformes: Potamotrygoninae. Zoomorphology. 2013; 142(2):181–91.
- **Araújo MLG, Charvet-Almeida P, Almeida MP, Pereira H.** Freshwater stingrays (Potamotrygonidae): status, conservation and management challenges. Information document AC. 2004; 20(8):1–06.
- **Barbosa ND, Wosnick N, Chaves AP, Giareta EP, Leite RD, Charvet P *et al*.** Ecotoxicology of Potamotrygoninae freshwater stingrays: bioaccumulation, toxicological risks, and conservation implications. Front Mar Sci. 2025; 12:1582093. https://doi.org/10.3389/fmars.2025.1582093
- **Beltrão H, Magalhães ERS, Benzaken ZS, Sousa RGC.** Trafficking of ornamental fish in the Brazilian amazon. Bol Inst Pesca. 2021; 47. https://doi.org/10.20950/1678-2305/bip.2021.47.e639
- **Betancur-R R.** Molecular phylogenetics supports multiple evolutionary transitions from marine to freshwater habitats in ariid catfishes. Mol Phylogenet Evol. 2010; 55(1):249–58. https://doi.org/10.1016/j.ympev.2009.12.018
- **Bloom DD, Lovejoy NR.** Molecular phylogenetics reveals a pattern of biome conservatism in New World anchovies (Family Engraulidae). J Evol Biol. 2012; 25(4):701–15. https://doi.org/10.1111/j.1420-9101.2012.02464.x
- **Bloom DD, Lovejoy NR.** On the origins of marine-derived freshwater fishes in South America. J Biogeogr. 2017; 44(9):1927–38. https://doi.org/10.1111/jbi.12954
- **Carvalho MR.** Neotropical stingrays: Family Potamotrygonidae. In: Last PR, White WT, Carvalho MR, Séret B, Stehmann MFW, Naylor GJP, editors. Rays of the World. Ithaca: Cornell University Press; 2016. p.619–55.
- **Carvalho MR, Lovejoy NR.** Morphology and phylogenetic relationships of a remarkable new genus and two new species of Neotropical freshwater stingrays from the Amazon basin (Chondrichthyes: Potamotrygonidae). Zootaxa. 2011; 2776(1):13–48. https://doi.org/10.11646/zootaxa.2776.1.2
- **Carvalho MR, Sabaj Pérez MH, Lovejoy NR.** *Potamotrygon tigrina*, a new species of freshwater stingray from the upper Amazon basin, closely related to *Potamotrygon schroederi* Fernandez-Yépez, 1958 (Chondrichthyes: Potamotrygonidae). Zootaxa. 2011; 2827(1):1–30. https://doi.org/10.11646/zootaxa.2827.1.1
- **Cooke GM, Chao NL, Beheregaray LB.** Marine incursions, cryptic species and ecological diversification in Amazonia: the biogeographic history of the croaker genus *Plagioscion* (Sciaenidae). J Biogeogr. 2012; 39(4):724–38. https://doi.org/10.1111/j.1365-2699.2011.02635.x
- **Dalgaard P.** R version 4.3.3 released [Internet]; 2024. Available from: https://stat.ethz.ch/pipermail/r-announce/2024/000699.html
- **Deynat P.** *Potamotrygon marina*e n. sp., a new species of freshwater stingrays from French Guiana (Myliobatiformes, Potamotrygonidae). Comptes Rendus Biologies, 2006; 329(7):483–93. https://doi.org/10.1016/j.crvi.2006.02.003
- **Ewart JC, Mitchell HC.** On the lateral sense organs of elasmobranchs. II. The sensory canals of the common skate (*Raja batis*). Trans R Soc Edinb. 1892; 37:87–105.
- **Ferreira FS, Lima FS, Seixas Filho JT, Silva ER, Sá MVC.** Use of clove oil to euthanize tropical ornamental fish. Acta Amaz. 2019; 49(3):228–33. https://doi.org/10.1590/1809-4392201802133

- **Fontenelle JP, Carvalho MR.** Systematic revision of the *Potamotrygon scobina* Garman, 1913 species-complex (Chondrichthyes: Myliobatiformes: Potamotrygonidae), with the description of three new freshwater stingray species from Brazil and comments on their distribution and biogeography. Zootaxa. 2017; 4310(1):1–63. https://doi.org/10.11646/zootaxa.4310.1.1
- **Fontenelle JP, Loboda TS, Kolmann M, Carvalho MR.** Angular cartilage structure and variation in Neotropical freshwater stingrays (Chondrichthyes: Myliobatiformes: Potamotrygonidae), with comments on their function and evolution. Zool J Linn Soc. 2018; 183(1):121–42. https://doi.org/10.1093/zoolinnean/zlx054
- **Fontenelle JP, Lovejoy NR, Kolmann MA, Marques FP.** Molecular phylogeny for the Neotropical freshwater stingrays (Myliobatiformes: Potamotrygoninae) reveals limitations of traditional taxonomy. Biol J Linn Soc. 2021b; 134(2):381–401. https://doi.org/10.1093/biolinnean/blab090
- **Fontenelle JP, Marques FPL, Kolmann MA, Lovejoy NR.** Biogeography of the neotropical freshwater stingrays (Myliobatiformes: Potamotrygoninae) reveals effects of continent-scale paleogeographic change and drainage evolution. J Biogeogr. 2021a; 48(6):1406–19. https://doi.org/10.1111/jbi.14086
- **Gandhi U.** “Estilización de una red fluvial con expresiones (QGIS3). [Internet]. 2021. Available from: https://www.qgistutorials.com/es/docs/3/river_styling_expressions.html#
- **Garman S.** On the lateral canal system of the Selachia and Holocephala. Bull Mus Comp Zool. 1888; 17:57–119.
- **International Union for Conservation of Nature (IUCN). Standards and Petitions Committee.** Guidelines for using the IUCN Red List Categories and Criteria. Version 14 [Internet]. Gland; 2024. Available from: https://www.iucnredlist.org/resources/redlistguidelines
- **Josse J, Husson F.** “missMDA: a package for Handling Missing Values in Multivariate Data Analysis.” J Statist Soft. 2016; 70(1):1–31. https://doi.org/10.18637/jss.v070.i01
- **Kolmann MA, Marques FP, Weaver JC, Dean MN, Fontenelle JP, Lovejoy NR.** Ecological and phenotypic diversification after a continental invasion in Neotropical freshwater stingrays. Integr Comp Biol. 2022; 62(2):424–40. https://doi.org/10.1093/icb/icac019
- **Larkin MA, Blackshields G, Brown NP, Chenna R, McGettigan PA, McWilliam H *et al*.** Clustal W and Clustal X version 2.0. Bioinformatics. 2007; 23(21):2947–48. https://doi.org/10.1093/bioinformatics/btm404
- **Le Bail PY, Covain R, Jégu M, Fisch-Muller S, Vigouroux R, Keith P.** Updated checklist of the freshwater and estuarine fishes of French Guiana. Cybium. 2012; 36(1):293–319.
- **Lo PC, Liu SH, Chao NL, Nunoo FK, Mok HK, Chen WJ.** A multi-gene dataset reveals a tropical New World origin and Early Miocene diversification of croakers (Perciformes: Sciaenidae). Mol Phylogenet Evol. 2015; 88:132–43. https://doi.org/10.1016/j.ympev.2015.03.025
- **Loboda TS, Carvalho MR.** Systematic revision of the *Potamotrygon motoro* (Müller & Henle, 1841) species complex in the Paraná-Paraguay basin, with description of two new ocellated species (Chondricthyes: Myliobatiformes: Potamotrygonidae). Neotrop Ichthyol. 2013; 11(4):693-737. https://doi.org/10.1590/S1679-62252013000400001
- **Lemopoulos A, Covain R.** Biogeography of the freshwater fishes of the Guianas using a partitioned parsimony analysis of endemicity with reappraisal of ecoregional boundaries. Cladistics. 2019; 35(1):106–24. https://doi.org/10.1111/cla.12341
- **Lovejoy NR.** Systematics of myliobatoid elasmobranchs: with emphasis on the phylogeny and historical biogeography of neotropical freshwater stingrays (Potamotrygonidae: Rajiformes). Zool J Linn Soc. 1996; 117(3):207–57. https://doi.org/10.1006/zjls.1996.0038

- **Lovejoy NR.** Stingrays, parasites, and neotropical biogeography: a closer look at Brooks et al.'s hypotheses concerning the origins of neotropical freshwater rays (Potamotrygonidae). Syst Biol. 1997; 46(1):218–30. https://doi.org/10.1093/sysbio/46.1.218
- **Lovejoy NR, Albert JS, Crampton WG.** Miocene marine incursions and marine/freshwater transitions: evidence from Neotropical fishes. J South Am Earth Sci. 2006; 21(1–2):5–13. https://doi.org/10.1016/j.jsames.2005.07.009
- **Lovejoy NR, Araújo ML.** Molecular systematics, biogeography and population structure of Neotropical freshwater needlefishes of the genus *Potamorrhaphis*. Mol Ecol. 2000; 9(3):259–68. https://doi.org/10.1046/j.1365-294x.2000.00845.x
- **Lovejoy NR, Bermingham E, Martin AP.** Marine incursion into South America. Nature. 1998; 396(6710):421–22. https://doi.org/10.1038/24757
- **Lovejoy NR, Collette BB.** Phylogenetic relationships of New World needlefishes (Teleostei: Belonidae) and the biogeography of transitions between marine and freshwater habitats. Copeia. 2001; 2001(2):324–38. https://doi.org/10.1643/0045-8511(2001)001[0324:PRONWN]2.0.CO;2
- **Lovejoy NR, Willis SC, Albert JS.** Molecular signatures of Neogene biogeographical events in the Amazon fish fauna. In: Hoorn C, Wesselingh FP, editors. Amazonia, landscape and species evolution: a look into the past. Blackwell Publishing, West Sussex, UK; 2009.
- **Lundberg JG, Kottelat M, Smith GR, Stiassny MLJ, Gill AC.** So many fishes, so little time: an overview of recent ichthyological discovery in continental waters. Ann Missouri Bot Gard. 2000; 87(1):26–62. https://doi.org/10.2307/2666207
- **Lujan NK, Armbruster JW.** The Guiana Shield. In: Albert JS, Reis RE, editors. Historical biogeography of Neotropical freshwater fishes. University of California Press; 2011. p.211–24. Available from: https://www.jstor.org/stable/10.1525/j.ctt1pp29c.17
- **Narayan K.** Climate change impacts on water resources in Guyana. IAHS Publication. 2006; 308–413.
- **Moro G.** Alimentação de *Potamotrygon signata* e *Potamotrygon orbignyi* (Chondrichthyes: potamotrygonidae) na bacia do rio Parnaíba. [PhD Dissertation]. João Pessoa: Universidade Federal da Paraíba; 2010.
- **Pedreros-Sierra TM, Ramírez-Pinilla MP.** Morphology of the reproductive tract and acquisition of sexual maturity in males of *Potamotrygon magdalenae* (Elasmobranchii: Potamotrygonidae). J Morphol. 2015; 276(3):273–89. https://doi.org/10.1002/jmor.20337
- **Reis RE, Albert JS, Di Dario F, Mincarone MM, Petry P, Rocha LA.** Fish biodiversity and conservation in South America. J Fish Biol. 2016; 89(1):12–47. https://doi.org/10.1111/jfb.13016
- **Rincon Filho G.** Aspectos taxonômicos, alimentação e reprodução da raia de água doce *Potamotrygon orbignyi* (Castelnau) (Elasmobranchii: Potamotrygonidae) no Rio Paraná-Tocantins. [Master Thesis]. Rio Claro: Universidade Estadual Paulista; 2006.
- **Rosa RS.** A systematic revision of the South American freshwater stingrays (Chondrichthyes: Potamotrygonidae) (Batoidei, Myliobatiformes, phylogeny, biogeography). The College of William and Mary; 1985.
- **Rosa RS, Carvalho MRD, Wanderley CDA.** *Potamotrygon boesemani* (Chondrichthyes: Myliobatiformes: Potamotrygonidae), a new species of Neotropical freshwater stingray from Surinam. Neotrop Ichthyol. 2008; 6(1):1–08. https://doi.org/10.1590/S1679-62252008000100001
- **Rutledge KM, Summers AP, Kolmann MA.** Killing them softly: ontogeny of jaw mechanics and stiffness in mollusk-feeding freshwater stingrays. J Morphol. 2019; 280(6):796–808. https://doi.org/10.1002/jmor.20984

- **da Silva JPCB.** Revisão taxonômica e morfológica do complexo *Potamotrygon orbignyi* (Castelnau, 1855) (Chondrichthyes: Myliobatiformes: Potamotrygonidae. [PhD Dissertation]. São Paulo: Universidade de São Paulo; 2010.
- **da Silva JPCB, Carvalho MR.** A taxonomic and morphological redescription of *Potamotrygon falkneri* Castex & Maciel, 1963 (Chondrichthyes: Myliobatiformes: Potamotrygonidae). Neotrop Ichthyol. 2011; 9(1):209–32. https://doi.org/10.1590/S1679-62252011000100021
- **da Silva JPCB, Carvalho MR.** Systematics and morphology of *Potamotrygon orbignyi* (Castelnau, 1855) and allied forms (Chondrichthyes: Myliobatiformes: Potamotrygonidae). Zootaxa. 2015; 3982(1):1–82. https://doi.org/10.11646/zootaxa.3982.1.1
- **da Silva JPCB, Rosa RS, Loboda TS, Lasso CA.** Taxonomy needs rigor: a response to Roberts' (2020). Zootaxa. 2021; 5052(4):597–600. https://doi.org/10.11646/zootaxa.5052.4.10
- **da Silva JPCB, Loboda TS.** *Potamotrygon marquesi*, a new species of neotropical freshwater stingray (Potamotrygonidae) from the Brazilian Amazon Basin. J Fish Biol. 2019; 95(2):594–612. https://doi.org/10.1111/jfb.14050
- **Souza LS, Armbruster JW, Werneke DC.** The influence of the Rupununi portal on distribution of freshwater fish in the Rupununi district, Guyana. Cybium. 2012; 36(1):31–43. https://doi.org/10.26028/CYBIUM/2012-361-004
- **Souza LS, Armbruster JW, Willink PW.** Connectivity of neotropical river basins in the central Guiana Shield based on fish distributions. Front For Glob Change. 2020; 3:8. https://doi.org/10.3389/ffgc.2020.00008
- **Taphorn DC, Liverpool E, Lujan NK, DoNascimiento C, Hemraj DD, Crampton WGR *et al*.** Annotated checklist of the primarily freshwater fishes of Guyana. PNAS. 2022; 168(1):1–95. https://doi.org/10.1635/053.168.0101
- **Toffoli D, Hrbek T, Araújo MLG, Almeida MP, Charvet-Almeida P, Farias IP.** A test of the utility of DNA barcoding in the radiation of the freshwater stingray genus *Potamotrygon* (Potamotrygonidae, Myliobatiformes). Genet Mol Biol. 2008; 31(1):324–36. https://doi.org/10.1590/S1415-47572008000200028
- **Torres Y, Faria VV, Charvet P.** Current status and future perspectives of Neotropical freshwater stingrays (Potamotrygoninae, Myliobatiformes) genetics. Environ Biol Fish. 2022; 105(8):1111–27. https://doi.org/10.1007/s10641-022-01320-x
- **Turner TF, McPhee MV, Campbell P, Winemiller KO.** Phylogeography and intraspecific genetic variation of prochilodontid fishes endemic to rivers of northern South America. J Fish Biol. 2004; 64(1):186–201. https://doi.org/10.1111/j.1095-8649.2004.00299.x
- **Wickham H.** ggplot2: elegant graphics for data analysis [Internet]. Springer-Verlag New York. 2016. Available from: https://ggplot2.tidyverse.org
- **Winemiller KO, López-Fernández H, Taphorn DC, Nico LG, Duque AB.** Fish assemblages of the Casiquiare River, a corridor and zoogeographical filter for dispersal between the Orinoco and Amazon basins. J Biogeogr. 2008; 35(9):1551–63. https://doi.org/10.1111/j.1365-2699.2008.01917.x
- **Willis SC, Nunes M, Montana CG, Farias IP, Orti G, Lovejoy NR.** The Casiquiare river acts as a corridor between the Amazonas and Orinoco river basins: biogeographic analysis of the genus *Cichla*. Mol Ecol. 2010; 19(5):1014–30. https://doi.org/10.1111/j.1365-294X.2010.04540.x
- **Yamanoue Y, Miya M, Doi H, Mabuchi K, Sakai H, Nishida M.** Multiple invasions into freshwater by pufferfishes (Teleostei: Tetraodontidae): a mitogenomic perspective. PLoS ONE. 2011; 6(2):e17410. https://doi.org/10.1371/journal.pone.0017410

AUTHORS' CONTRIBUTION

Devya Hemraj-Naraine: Data curation, Formal analysis, Investigation, Methodology, Visualization, Writing-original draft, Writing-review and editing.

João Pedro Fontenelle: Conceptualization, Formal analysis, Investigation, Methodology, Resources, Software, Writing-review and editing.

Astrid Acosta-Santos: Data curation, Investigation, Writing-review and editing.

Nathan R. Lovejoy: Conceptualization, Funding acquisition, Writing-review & editing

Elford Liverpool: Investigation, Writing-review & editing

Matthew A. Kolmann: Conceptualization, Formal analysis, Funding acquisition, Investigation, Methodology, Project administration, Supervision, Writing-review and editing.

FUNDING INFORMATION

The authors were funded by Conselho Nacional de Desenvolvimento Científico e Tecnológico – CNPq (CO, grants #207384/2014–2). Friday Harbor Laboratories Post-Doctoral Fellowship, an NSF Post-Doctoral Research Fellowship (PRFB 1712015), Rufford Foundation Small Grant and a Natural Sciences and Engineering Research Council of Canada discovery grant. This project was partially funded by a Rufford Small Grant and University of Louisville start-up funds to MAK.

ETHICAL STATEMENT

Not applicable.

DATA AVAILABILITY STATEMENT

The datasets generated during the current study are available in the GenBank repository, https://doi.org/10.1111/jbi.14086.

AI STATEMENT

The authors did not use any AI-assisted technologies in the creation of this manuscript or its figures.

COMPETING INTERESTS

The authors declare no competing interests.

SUPPLEMENTARY MATERIAL

Supplementary material **S1**

HOW TO CITE THIS ARTICLE

- **Hemraj-Naraine D, Fontenelle JP, Acosta-Santos A, Lovejoy NR, Liverpool E, Kolmann MA.** A new species of freshwater stingray (Myliobatiformes: Potamotrygoninae) from northern South America. Neotrop Ichthyol. 2026; 24(1):e250178. https://doi.org/10.1590/1982-0224-2025-0178

Neotropical Ichthyology

OPEN ACCESS

SBI
Official Journal of the
Sociedade Brasileira de Ictiologia